ALMA MATER STUDIORUM
UNIVERSITÀ DI BOLOGNA

SCUOLA DI INGEGNERIA E ARCHITETTURA

SEDE DI FORLÌ

CORSO DI LAUREA IN INGEGNERIA AEROSPAZIALE

CLASSE L9

Design of a return circuit for an open loop wind tunnel

ELABORATO FINALE DI LAUREA IN

LABORATORIO DI AERODINAMICA SPERIMENTALE

Candidate
Edoardo Foschi

Supervisor
Chiar.mo Alessandro
Talamelli

Accademic Year 2019/2020

”We feel that even when all possible scientific questions have been answered, the problems of life remain completely untouched. Of course there are then no questions left, and this itself is the answer.”
Ludwig Wittgenstein, *Tractatus logico-philosophicus*.

Abstract

This work is about the design of two different solutions of a return circuit for the subsonic open loop wind tunnel of the University of Bologna placed in the laboratory of aerodynamics. The possibility of realizing a return circuit was born from the idea of moving the current wind tunnel to a different place. Realizing a closed-type wind tunnel could permit a better installation with reduced costs since the starting point of the project is an existing tunnel. Two different design solutions are shown in order to satisfy different conditions of allocation: one model has vertical development, the other has horizontal development. The conceptual phase is followed by a study of the pressure losses in order to evaluate which design solution could be the best.

Sommario

Il presente elaborato propone due diverse soluzioni costruttive di un circuito di chiusura per la galleria del vento subsonica a ciclo aperto presente presso il laboratorio di Aerodinamica dell'Università di Bologna. La possibilità di realizzare un circuito di chiusura nasce dall'idea di spostare l'attuale galleria in un luogo differente. Realizzarre una galleria a ciclo chiuso permetterebbe un impianto di maggior qualità e partendo da una galleria già esistente i costi sarebbero contenuti. Sono presentate due soluzioni costruttive , una che si sviluppa sul piano verticale e una su quello orizzantale, in base a differenti ambienti di collocamento. La fase concettuale del progetto è seguita dalla stima delle perdite di carico indotte dai componenti, necessaria per valutare quale soluzione sarebbe di migliore impiego.

Acknowledgements

First of all I am grateful to professor Alessandro Talamelli who was able to offer me an interesting and challenging project work for my thesis. Throughout it I was able to prove myself and to grow not only my knowledge but my ability to believe in myself.

I want to show gratitude for my parents, Folgora and Giorgio, who always helped me and let me free to follow my desires. I have never found myself alone thanks to the support of my family: they will always be here.

Special thanks go to all my friend who followed me during the recent years and from whom I will always have support and something to learn.

Introduction

Wind tunnels are essential installations to realize experiments of aerodynamics. The fundamental equations of aerodynamics do not have an exact analytic solution so that experimental methods are necessaries to obtain useful information to solve aerodynamic problems. Wind tunnels with a closed return are specifically the best way to acquire valid data in the face of being more expensive than an open-type solution.

A subsonic open return wind tunnel is placed in the laboratory of aerodynamics of the University of Bologna. The costs of realizing a closed wind tunnel are reduced if it is used the above-mentioned tunnel as a starting point. After have been drawn a 3D model of the open wind tunnel in a CAD software, two different models are deigned in order to have different solutions that can satisfy different places of allocation. The place of positioning of the wind tunnel imposes the limits of the project forcing to adopt different design solutions and studies of the ranges of each element. Since the purpose of the circuit is to guarantee a steady air flow in the test section, the design phases are the most delicate. Errors it he project can compromise the quality and the validity of the experiments taken due to turbulence, separation and other phenomenons that could occur to the internal fluid.

It is necessary to realize a study of the pressure losses after the design phase to understand which of the two different models shown could be the best solution to adopt and to evaluate the new velocity achievable in the test section using the same fan of the current open wind tunnel.

Contents

Acknowledgements **iii**

Introduction **iv**

1 Wind Tunnels **1**
- 1.1 Purpose . . . 1
- 1.2 Parameters for similarity . . . 1
- 1.3 Types of wind tunnels . . . 4
  - 1.3.1 Open Return Wind Tunnels . . . 5
  - 1.3.2 Closed Return Wind Tunnels . . . 6
- 1.4 Principal Components . . . 7
  - 1.4.1 Test section . . . 7
  - 1.4.2 Diffuser . . . 8
  - 1.4.3 Nozzle . . . 14

2 Design **17**
- 2.1 Open loop tunnel . . . 17
  - 2.1.1 Chamber of calm . . . 17
  - 2.1.2 Nozzle . . . 18
  - 2.1.3 Test section . . . 18
  - 2.1.4 Diffuser . . . 18
  - 2.1.5 Fan . . . 19
- 2.2 Vertical design . . . 20
  - 2.2.1 Corners . . . 20
  - 2.2.2 Shape adapter . . . 22
  - 2.2.3 Diffuser . . . 24
  - 2.2.4 Complete design of the return circuit . . . 25
- 2.3 Horizontal design . . . 26

2.3.1 Corners 26
2.3.2 Shape adapter 27
2.3.3 Constant area duct 28
2.3.4 Diffusers 29
2.3.5 Complete design of the return circuit 31

3 Pressure Losses **32**
3.1 Energy Consideration 32
3.2 Energy Losses 33
3.3 Constant-area section 35
3.4 Diffuser 38
3.5 Nozzle 41
3.6 Corners 42
3.7 Honyecombs 43
3.8 Screens 44
3.9 Total losses 47
3.9.1 Vertical design 47
3.9.2 Horizontal design 51

4 Conclusions **55**

A Vertical design **57**

B Horizontal design **63**

List of Figures

1.1 Scheme of an open loop wind tunnel 5
1.2 Scheme of a closed loop wind tunnel extracted from [1] 6
1.3 Internal flow in a duct, extracted from [2] 7
1.4 Scheme of diffusers: (a) flat-walled; (b) conical 8
1.5 Diffuser performance: (a) ideal pattern with good performance; (b) actual measured pattern with boundary layer separation and resultant poor performance. extracted from [2] 10
1.6 Flow regimes in subsonic straight wall two-dimensional diffusers with steady inlet 11
1.7 Map of the performance of a flat-walled diffuser, extracted from [2] 13
1.8 Map of the performance of a conical diffuser, extracted from [2] . 13
1.9 Velocity profiles inside a nozzle, extracted from [3] 15
1.10 Concave-convex shape of a nozzle, extracted from [3] 16

2.1 Open loop wind tunnel placed in the hangar 17
2.2 Fan 19
2.3 Rendering 3D of the close wind tunnel 20
2.4 Corners 3 and 4 21
2.5 Corners 1 and 2 22
2.6 Design of the shape adapter 23
2.7 Two different type of shape possible: a) Simple contraction; b) Concave-convex 23
2.8 Design of the diffuser 24
2.9 Design of the complete design of the return circuit 25
2.10 Rendering 3D of the close wind tunnel 26
2.11 3D rendering with the corner with circular area section 27
2.12 Design of last two corners with the diffuser between them 27
2.13 Design of the shape adapter 28

2.14 Design of the second side of the return circuit with the element of constant cross-sectional area 29
2.15 Design of the two diffusers 30
2.16 Design of the complete design of the return circuit 31

3.1 Moody diagram 37
3.2 Coeff. of pressure recovery for a diffuser with tailpipe such that $4 < L_d/D_{H2} < 8$, extracted from [3] 40
3.3 Scheme of corners with and without turning vanes, extracted from [4] 42
3.4 Scheme of turning vanes 43
3.5 Scheme of the mail of honeycombs 44
3.6 Scheme of the flow inside the screens, extracted from [5] 45
3.7 Scheme of the evolution of the velocity distribution inside the screen with the variance of the porosity; a) $\beta = 0,75$, $K_l = 0.5$; b) $\beta = 0,53$, $K_l = 2$ c) $\beta = 0.20$, $K_l = 15$, extracted from [3] . . 46
3.8 Total losses 48
3.9 Velocity distribution 48
3.10 Static pressure 49
3.11 Dynamic pressure 49
3.12 Total pressure 50
3.13 Total losses 52
3.14 Velocity distribution 52
3.15 Static pressure 53
3.16 Dynamic pressure 53
3.17 Total pressure 54

Chapter 1

Wind Tunnels

1.1 Purpose

A wind tunnel is an installation used in order to realize aerodynamic experiments. A stream of air can be created internally in compliance with adjustable parameters, such as velocity, pressure and temperature. The object of studies is placed inside of it and experiments to understand its behaviour in such condition are taken, measuring the forces and the pressures acting on the body throughout specific sensors.

Although the progresses made throughout computational fluid dynamics, wind tunnels are still used to get experimental information useful for solving aerodynamic problems. The main reason is that the Navier-Stokes equations, which are the fundamental equations of aerodynamics, do not have an exact analytic solution. Approximate solutions can be obtained with CFD but they do not have accuracy since the starting point of them is a simplified model therefore it is better to realize experimental studies too. Wind tunnels make it possible to use models that can be prepared early in design cycles, they include the full complexity of real fluid flow, and they can provide large amounts of reliable data, therefore they are the most rapid, economical, and accurate means for conducting aerodynamic research and obtaining aerodynamic data to support design decisions.

1.2 Parameters for similarity

Since the primary activity of wind tunnels is conducting experiments using scale models, parameters for similarity must be considered in order to have a valid

model. The results of principal interest are the dimensionless coefficients that appear in these fluid dynamics equations: the Reynolds number, the Mach number, and the Froude number. When a body moves through a fluid, forces arise that are due to the viscosity of the fluid, its inertia, its elasticity, and gravity. These forces are represented directly by the various terms in the Navier-Stokes equation. The inertia force is proportional to the mass of air affected and the acceleration given that mass. Thus, while it is true that a very large amount of air is affected by a moving body, the inertia force is the result of giving a constant acceleration an effective volume of air. Let this effective volume of air he kl^3, where l is a characteristic length of the body and k is a constant for the particular body shape. Then we may write for the inertia force:

$$F_i = \frac{\rho l^3 V}{t} \tag{1.1}$$

Subsituting l/V for t:

$$F_i = \frac{\rho l^3}{l/V} = \rho l^2 V^2 \tag{1.2}$$

The viscous force, according to its definition, may be written as:

$$F_v \sim \mu V l \tag{1.3}$$

The gravity force is proportional to the volume of the body, which in turn is proportional to the cube of the reference length. The gravity force may be written:

$$F_g = \rho l^3 g \tag{1.4}$$

where g is the acceleration of gravity. The gravity force term in the Navier-Stokes equation is the force on the fluid but is not the gravity force on the body. So it is necessary to introduce the equations of motion of the body along with the equations of motion of the fluid to carry out a formal non-dimensionalization for the case of a fully coupled system of the motion of the body moving under the influence of the fluid and gravitational forces. In this dissertation the gravity force on the body is considered to have the same form as the gravity force on the fluid but with a different constant of proportionality.

The elastic force may be considered to be:

$$F_e \sim p l^2 \tag{1.5}$$

The speed of sound a in a fluid is related to pressure and density according to:

$$a^2 \sim \frac{p}{\rho} \tag{1.6}$$

so that we may write:

$$F_e \sim \rho a^2 l^2 \tag{1.7}$$

Dividing the inertia force by each of the others gives three force ratios that are the same forms as the dimensionless coefficients :

$$Re = \frac{F_i}{F_v} = \frac{p}{\mu} Vl \tag{1.8}$$

$$Ma = \frac{F_i}{F_e} = \frac{V}{a} Vl \tag{1.9}$$

$$Fr = \sqrt{\frac{F_i}{F_g}} = \sqrt{\frac{V^2}{lg}} \tag{1.10}$$

For wind tunnel experiments, the Froude number is an important similarity parameter only for dynamic tests in which model motion as well as the aerodynamic forces are involved. For experiments in which the model is held stationary during data gathering, the Reynolds number and Mach number are the significant similarity parameters. If a model experiment has the same Reynolds and Mach numbers as the full-scale application, then the model and the full-scale flows will be dynamically similar. The non-dimensional functions for fluid velocity components, pressure coefficient, density, viscosity, and temperature will then be the same for the model and the full-scale flows. In turn the force and moment coefficients will be the same for the model and full-scale flows. Under these conditions, the forces developed by the model can be directly related to the forces on the full-scale article by multiplying the force coefficients obtained in the experiment using the model by the factor $\frac{1}{2} p_\infty V_\infty^2 l^2$ with the values of parameters in the factor corresponding to full scale. The moments developed by the model can be directly related to the moments on the full-scale article by multiplying the moment coefficients obtained in the experiment using the model by the factor $\frac{1}{2} p_\infty V_\infty^2 l^2$ with the values in the factor corresponding to full scale.

It is seldom possible to match both Reynolds number and Mach number to full scale in a model experiment. In fact, it is frequently the case that neither Reynolds

number nor Mach number can be matched. Choices must then be made on the basis of which parameter is known to be most important for the type of flow situation under consideration. Despite of that, the wind tunnel still is one of the most useful tools for aerodynamic studies. The more complex the flow phenomena involved, the more important will be the role of the wind tunnel. From the scaling relations it follows that the force on a body of a particular shape for which the flow characteristics are a function only of Reynolds number is the same regardless of the combination of size and speed that is used to produce the particular Reynolds number if the fluid, its temperature, and the free-stream pressure are unchanged. This can be seen by writing the expression for a force component; for example the drag:

$$D = \frac{1}{2} p_\infty V_\infty^2 l^2 C_d\left(Re\right) = \frac{1}{2} \frac{p_\infty V_\infty^2 l^2}{\mu_\infty^2} \frac{\mu_\infty^2}{p_\infty^2} C_d\left(Re\right) \tag{1.11}$$

That indicates that increasing the velocity smaller models can be used with a still valid result.

1.3 Types of wind tunnels

A first division throughout the Mach number can be made:

- subsonic tunnels with incompressible fluids (M $<$ 0.3)
- subsonic tunnels with compressible fluids (0.3 $<$ M $<$ 0.8)
- transonic tunnels (0.8 $<$ M $<$ 1.2)
- supersonic tunnels (1.2 $<$ M $<$ 5)
- hypersonic tunnel (M $>$ 5)

Other two basic-types of wind tunnels are open circuit and closed circuit. The air flowing through an open circuit tunnel follows an essentially straight path from the entrance through a contraction to the test section, followed by a diffuser, a fan section, and an exhaust of the air. The air flowing in a closed return wind tunnel recirculates continuously with little or no exchange of air with the exterior.

1.3.1 Open Return Wind Tunnels

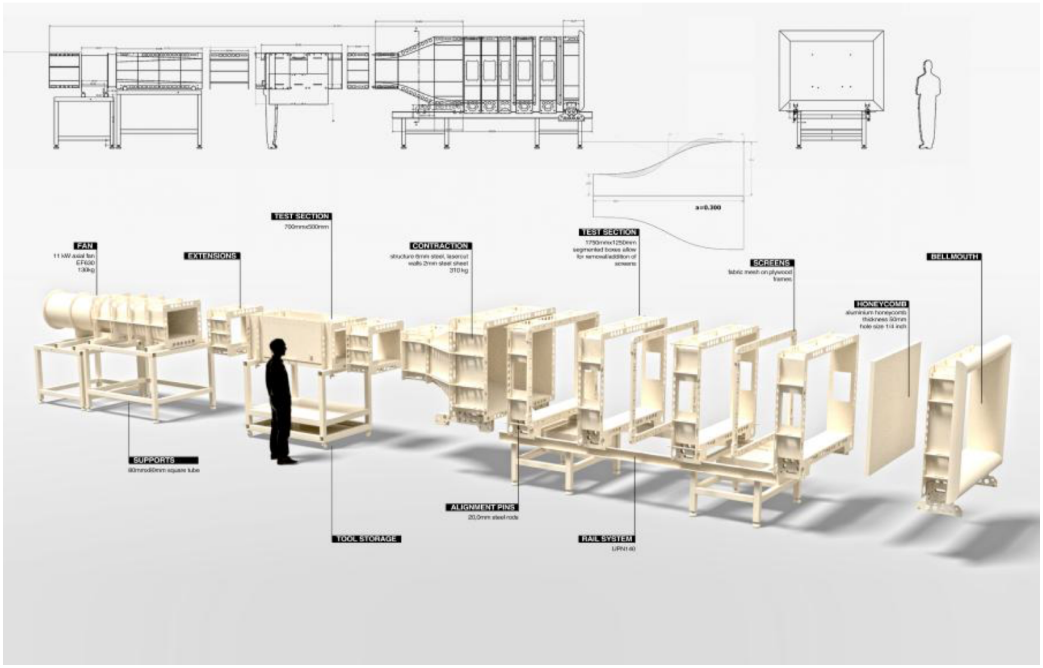

Figure 1.1: Scheme of an open loop wind tunnel

Advantages

1. The cost of construction is much less than a closed-type.
2. If one intends to run internal combustion engines or do extensive flow visualization via smoke, there is no purging problem provided both inlet and exhaust are open to the atmosphere.

Disadvantages

1. It may require extensive screening at the inlet to get high-quality flow especially if the inlet and exhaust is open to the atmosphere, when wind and cold weather can affect operation.
2. For a given size and speed the tunnel will require more energy to run. This is usually a factor only if the tunnel has a high utilization rate.

3. In general, open circuit tunnels tend to be noisy. This may cause environmental problems, limit hours of operations, requiring extensive noise treatment of the tunnel and surrounding room.

1.3.2 Closed Return Wind Tunnels

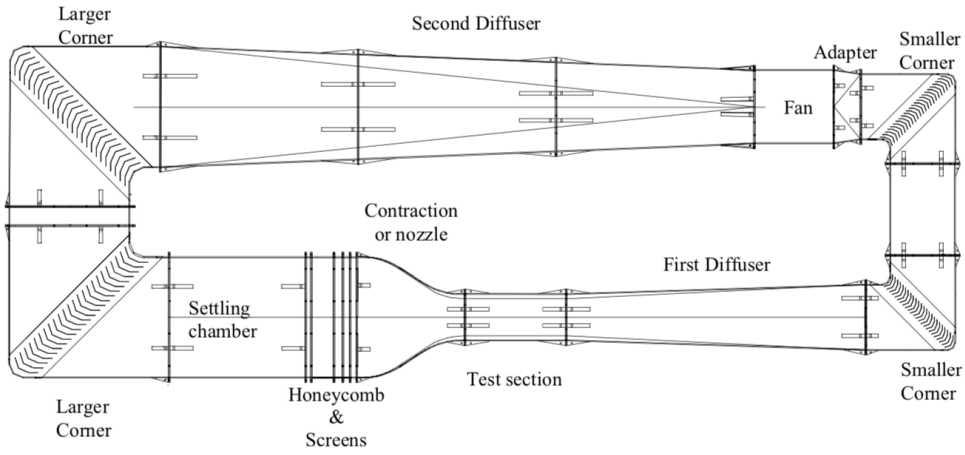

Figure 1.2: Scheme of a closed loop wind tunnel extracted from [1]

Advantages

1. Through the use of corner turning vanes and screens, the quality of the flow can be well controlled and it will be independent of other activities in the building and weather conditions.

2. Less energy is required for a given test-section size and velocity thanks to the recovery of pressure inside the circuit.

3. There is less environmental noise when operating.

Disadvantages

1. The initial cost is higher due to return ducts and comer vanes.

2. A way to purge tunnel must be found if it is used widely for smoke flow visualization experiments or running of internal combustion engines.

Opportunities for the University of Bologna

Since the laboratory of experimental aerodynamics of the University of Bologna has already an open loop tunnel the cost of production will be contained if the design starts from it. This investment could improve the capability of the facility increasing the velocity of the flow in the test section for the given fan power and the quality of the stream reducing turbulence problems.

1.4 Principal Components

1.4.1 Test section

The test section is the most important part of the wind tunnel since the experiments are realized internally. All the other parts of the wind tunnel are studied in order to guarantee the desirable flow in the test section.

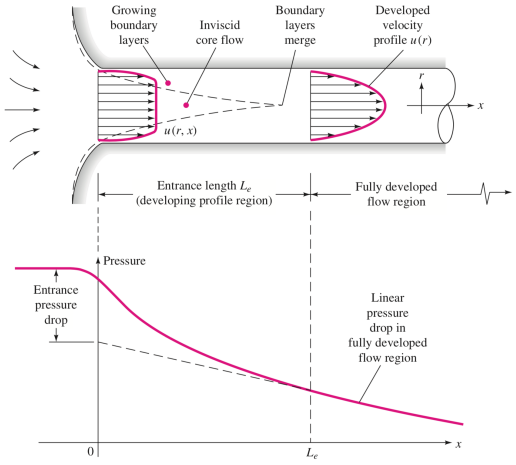

Figure 1.3: Internal flow in a duct, extracted from [2]

The length of a test section must be included between 0.5 times and 3 times its hydraulic diameter. This choice is due to the fact that the air flow exiting from the nozzle needs at least 0.5 times the hydraulic diameter to become uniform. Furthermore a test chamber too much long could introduce the problem of separation during the exit from the chamber. There is not a unique way to design a test sec-

tion, considerations of the shape and of using a open or closed section are made based on the purpose of the wind tunnel.

1.4.2 Diffuser

Since the power losses at any point in the tunnel are expected to vary as the speed cubed, the purpose of the diffuser is to reduce the speed with as little energy loss as possible. Minimum energy loss corresponds to maximum pressure recovery. It is generally desirable to reduce the speed in the shortest possible distance without incurring flow separation. This will obtain good efficiency and will help to reduce construction costs by reducing the overall size of the tunnel shell. Obtaining good performance from the diffuser is critical to the success of the tunnel. Diffusers are sensitive to design errors that may cause either intermittent separation or steady separation. Such separations can be hard to localize but can cause vibrations, oscillating fan loading, oscillations in test-section velocities, and increased losses in the tunnel downstream of their origin.

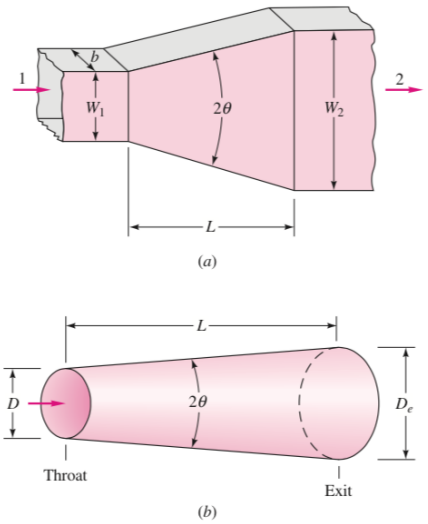

Figure 1.4: Scheme of diffusers: (a) flat-walled; (b) conical

The primary parameters for a diffuser are the equivalent conical expansion angle and the area ratio. Consider a conical diffuser with a radius R_1 at the entrance, radius R_2 at the exit and length L. The equivalent conical angle is defined as fol-

lows. Let AR be A_2/A_1. Then the equivalent conical expansion angle is given by:

$$\theta_c = arctg\left(\frac{R_2 - R_1}{L}\right) = arctg\left(\frac{1}{2}\frac{\sqrt{A_R}-1}{\frac{L}{D_1}}\right) \tag{1.12}$$

To understand the performance of the diffuser, the behaviour of the internal flow must be considered. Neglecting losses and gravity effects, the incompressible Bernoulli equation predicts that:

$$p + \frac{1}{2}\rho V^2 = p_0 = const \tag{1.13}$$

where p_0 is the stagnation pressure the fluid would achieve if the fluid were slowed to rest $V = 0$ without losses.

The basic output of a diffuser is the *pressure recovery coefficient* C_p defined as:

$$C_p = \frac{p_2 - p_1}{p_{01} - p_1} \tag{1.14}$$

Higher C_p means better performance.

Considering a flat-walled diffuser where section 1 is the inlet and section 2 the exit. Application of Bernoulli's equation to this diffuser predicts that:

$$p_{01} = p_1 + \frac{1}{2}\rho V_1^2 = p_2 + \frac{1}{2}\rho V_2^2 = p_{02} \tag{1.15}$$

$$C_{p_frictionless} = 1 - \left(\frac{V_2}{V_1}\right)^2 \tag{1.16}$$

Meanwhile, steady one-dimensional continuity would require that:

$$Q = V_1 A_1 = V_2 A_2 \tag{1.17}$$

Combining the two equations we can write the performance in terms of the *area ratio* $AR = A_2/A_1$ which is a basic parameter in diffuser design:

$$C_{p_frictionless} = 1 - (AR)^2 \tag{1.18}$$

A typical design would have $AR = 5:1$, for which the last equation predicts $C_p = 0.96$, or nearly full recovery. Actually the measured values of C_p through experiments for this area ratio are only as high as 0.86 and can be as low as 0.24.

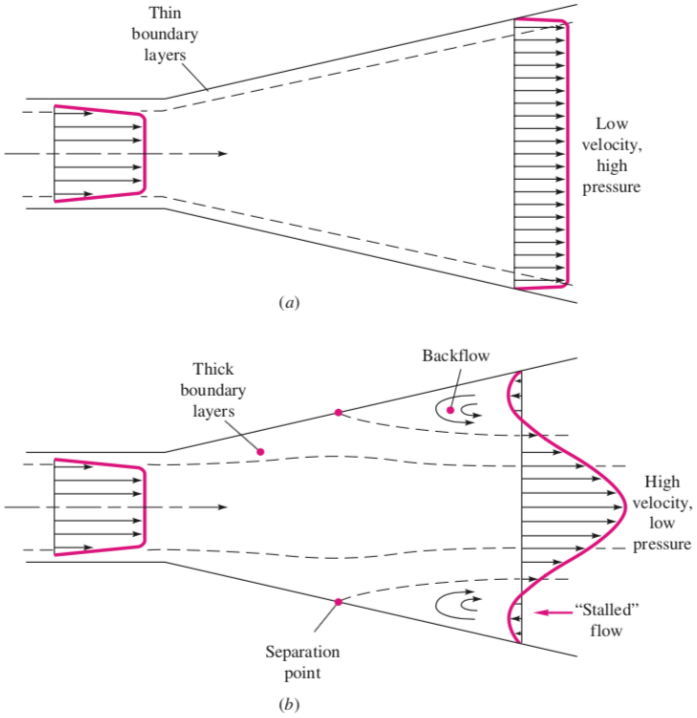

Figure 1.5: Diffuser performance: (a) ideal pattern with good performance; (b) actual measured pattern with boundary layer separation and resultant poor performance. extracted from [2]

This discrepancy is due to flow separation, as shown in Fig. 1.5. The increasing pressure in the diffuser is an unfavorable gradient, which causes the viscous boundary layers to break away from the walls and greatly reduces the performance. As an added complication to boundary layer separation, the flow patterns in a diffuser are highly variable. A complete stability map of diffuser flow patterns was published by Fox and Kline, as shown in Fig.1.6 for a flat-walled diffuser.

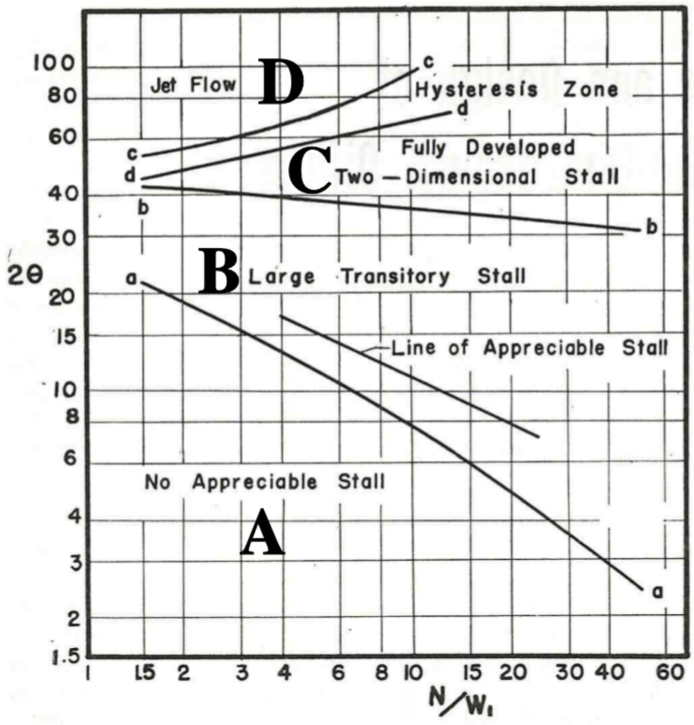

Figure 1.6: Flow regimes in subsonic straight wall two-dimensional diffusers with steady inlet

There are four basic regions. Below line *aa* there is the *A* zone where the flow is steady and viscous, there is not separation and it has moderately good performance. Flow separation could be reach anyway if the half-angle is greater than 6°. In *B* there is a transitory stall pattern with strongly unsteady flow. Best performance occurs in this region. In the third pattern *C* there is steady bistable stall from one wall only and the performance is poor. In *D* there is *jet flow*, where the wall separation is so pervasive that the mainstream behaves as the walls do not exist and simply passes on through at nearly constant area. Performance is extremely poor in this region.

Dimensional analysis of a flat-walled or conical diffuser shows that C_p should depend on the following parameters:

- The following geometric parameters:
  - Area ratio $AR = A_2/A_1$ or $(D_e/D)^2$

  - Divergence angle 2θ
  - Slenderness L/W_1 or L/D

- Inlet Reynolds number $Re_1 = V_1 W_1/\nu$ or $Re_1 = V_1 D/\nu$
- Inlet Mach number $Ma_1 = V_1/a_1$
- Inlet boundary layer blockage factor $B_1 = A_{BL}/A_1$, where A_{BL} is the wall area blocked, or displaced, by the retarded boundary layer flow in the inlet (typically B_1 varies from 0.03 to 0.12)
- Aspect ratio $AS = b/W_1$ (additional parameter required to describe cross section for a flat-walled diffuser)

In practical machinery applications could happen other effects, such as inlet turbulence, inlet swirl, inlet profile vorticity, superimposed pulsations, and downstream obstruction. In general can be determined empirically that performance decreases with blockage and it is approximately the same for both flat-walled and conical diffusers. In all cases, the best conical diffuser is 10 to 80 percent longer than the best flat-walled design. Therefore, if length is limited in the design, the flat-walled design will give the better performance depending on duct cross section. The experimental design of a diffuser is an successful attempt to minimize the undesirable effects of adverse pressure gradient and flow separation.

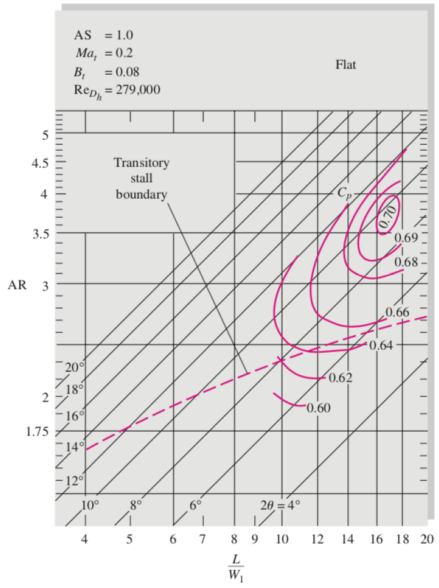

Figure 1.7: Map of the performance of a flat-walled diffuser, extracted from [2]

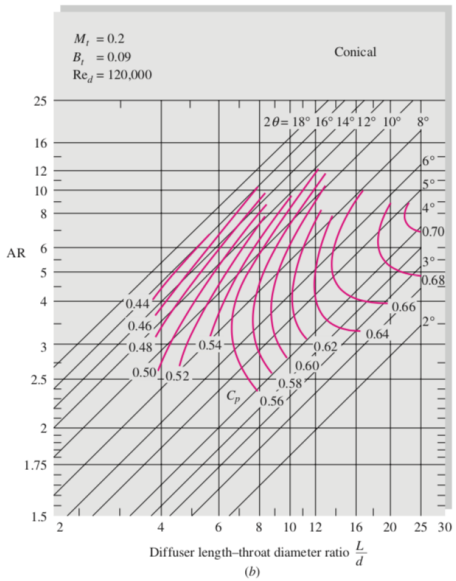

Figure 1.8: Map of the performance of a conical diffuser, extracted from [2]

1.4.3 Nozzle

The nozzle accelerates the flow from the settling chamber to the test section, further reducing any variations in velocity. In a wind tunnel the flow velocity and its uniformity within the test chamber cross-section depend on the nozzle's design. The nozzle exit cross-section dimensions and shape are identical to the test chamber ones since they are joined together. The nozzle area ratio should be as large as possible to reduce the total-pressure loss through the screens mounted between the settling chamber and the nozzle. Normally, the nozzle inlet/outlet cross-section area ratio should be in the range 6 - 10. Area ratios greater than 10 lead to excessive inlet dimensions while area ratios less than 6 lead to high pressure loss through the screens.

The increase of the velocity can be determined by the equation of mass conservation from the eulerian point of view (where Σ is the volume of control):

$$\int_{\Sigma} \left(\frac{D\rho}{Dt} + \rho div(V) \right) d\Sigma = 0 \tag{1.19}$$

Considering $\rho = cost$ since the flow is incompressible and using the divergence theorem, it can be written:

$$\int_{S} n\,(\rho V)\, dS = 0 \tag{1.20}$$

The flow direction is perpendicular to the versor n in the lateral wall and parallel to the sections of entrance A_1 and exit A_2, the equation assumes the form of:

$$\int_{A_1} \rho V_1\, dS_1 \int_{A_2} \rho V_2\, dS_2 = 0 \tag{1.21}$$

If the viscuos effects are neglected so that $V_1 = const$ and $V_2 = const$, we obtain:

$$V_2 \simeq V_1 \frac{A_1}{A_2} = V_1 CR \tag{1.22}$$

where CR is the *contraction ratio* that can be written as:

$$CR = \frac{D_1^2}{D_2^2} \tag{1.23}$$

The reduction of turbulence in the entering section and exit section depends on this parameter, as shown in the following equations:

$$\frac{u_2'}{U_2} = \frac{u_1'}{CR^2 U_1} \tag{1.24}$$

$$\frac{v_2'}{U_2} = \frac{v_1'}{\sqrt{CR}U_1} \tag{1.25}$$

The stream at the beginning of the nozzle starts to increase on average but the effects pressure gradient are dominant. As a consequence the velocity at the walls reaches the relative minimum at the beginning of the nozzle and a relative maximum before the exit section. Between these points and the extremes of the nozzle there is a recover of static pressure meaning the stream is exposed to an adverse gradient. This situation can lead to the separation of boundary layers.

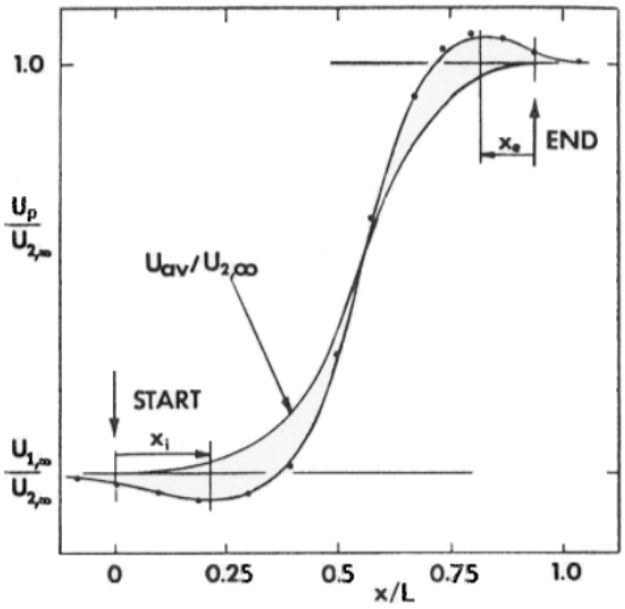

Figure 1.9: Velocity profiles inside a nozzle, extracted from [3]

To avoid this circumstance it is better to realize a geometry of the profile such that the critic entering section is more developed in length in order to minimize the increase of the static pressure.

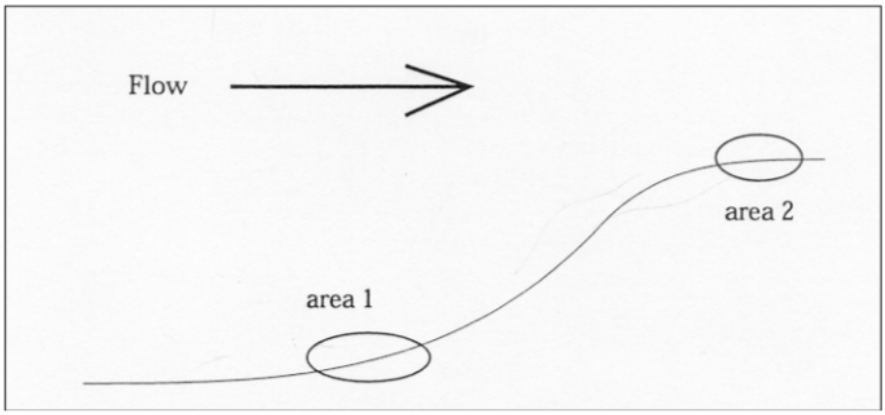

Figure 1.10: Concave-convex shape of a nozzle, extracted from [3]

Chapter 2

Design

2.1 Open loop tunnel

An open loop subsonic wind tunnel is placed in the laboratory of experimental aerodynamic of the University of Bologna. To realize a return circuit means to improve the quality of the air flow inside the wind tunnel and to obtain a higher velocity in the section with equal fan power.

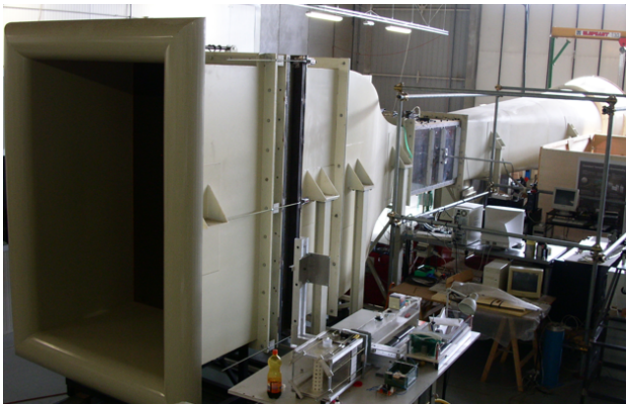

Figure 2.1: Open loop wind tunnel placed in the hangar

2.1.1 Chamber of calm

A chamber of calm is placed at the beginning of the wind tunnel in order to make homogeneous the air flow. Potential components of swirl and turbulence are

deleted throughout honeycombs and screens. Since these elements insert losses of power proportionally with the square of the velocity, they are placed at the beginning of the tunnel where the flow is almost calm.

Chamber of calm	
Length	2200 mm
Height	2235 mm
Width	1490 mm
Cross-sectional Area	2.22 m^2

2.1.2 Nozzle

The quality of the flow in the section is strongly conditioned by the presence of the nozzle, which realize the acceleration of the flow entering.

Nozzle	
Entering area	3.33 m^2
Exit area	0.53 m^2
Coeff. of contractionCR	6.23
Length	2490 mm
Equivalent conic angle θ_e	12.2 $^\circ$

2.1.3 Test section

The test section is the most important part of the wind tunnel since is where the experiments take place. The flow must respect all the parameters inside in order to obtain correct results.

Test Chamber	
Length	1830 mm
Height	900 mm
Width	590 mm
Max Velocity	50 $(m/s)^2$

2.1.4 Diffuser

After the test section a diffuser helps to minimize the required energy to speed up the flow.

Diffuser	
Entering area	0.531 m^2
Exit area	2.54m^2
Length	9.91 m
Equivalent conic angle θ_e	3.14 °

2.1.5 Fan

The fan realizes a rise in pressure as the flow passes through the section. The increase in pressure provided must be equal to the pressure losses throughout all other sections of the wind tunnel at any given steady flow operating condition. The fan in this gallery is a pulling type in order to avoid introduction of swirl and turbulence components in the air before the flow enters the test section.

Fan duct	
Length	550 mm
Diameter	1.8 m
Cross-sectional area	2.545 m^2

Figure 2.2: Fan

A fan outlet is placed at the end of this section. To realize the return circuit it is removed so it is not shown in the models.

2.2 Vertical design

The first model shown has a vertical development in order to adapt the wind tunnel to a narrow place. Height is the only limit of the project. This situation leads to realize all the expansion of the flow in one single diffuser in the return circuit, placed between the second and the third corner. Since there are not limits in length, new components can be added after the fan section of the open loop wind tunnel. The more suitable is a change adapter in order to not have circular corners, which are more expensive and difficult to be realized.

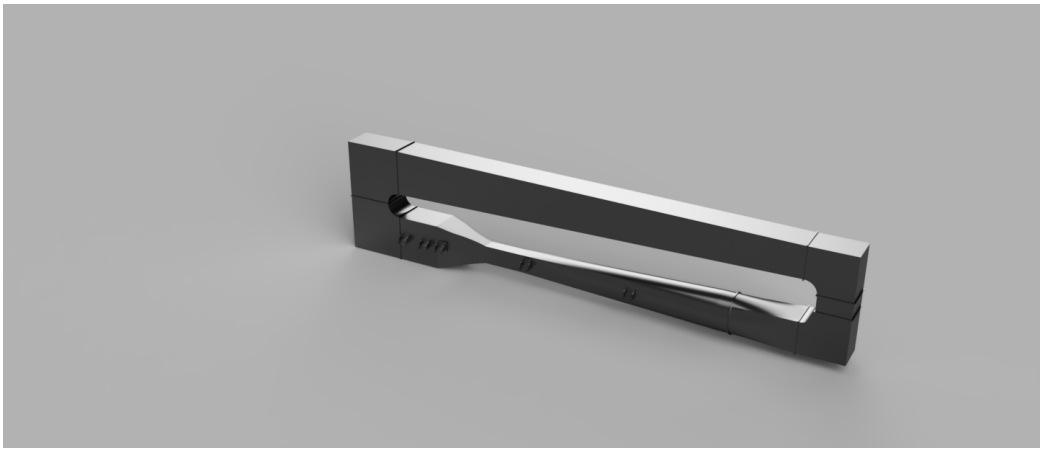

Figure 2.3: Rendering 3D of the close wind tunnel

2.2.1 Corners

Since height is the limit of the project, the starting parts of the return circuit to be designed are the corners joined to the chamber of calm. Corners with constant area section have been chosen in order to simplify the building phases and to minimize the costs. Since 2235 *mm* is the height of the chamber of calm and 600 *mm* is good value for the radius of connection of corners wind tunnel, the minimum height of the return circuit possible is:

$$H = (H_{chamber} + Radius) * 2 = 5670mm \tag{2.1}$$

The cross-sectional area of these corners is the same of the chamber of calm:

$$A_c = H_{chamber} * W_{chamber} = 3.33 mm^2 \tag{2.2}$$

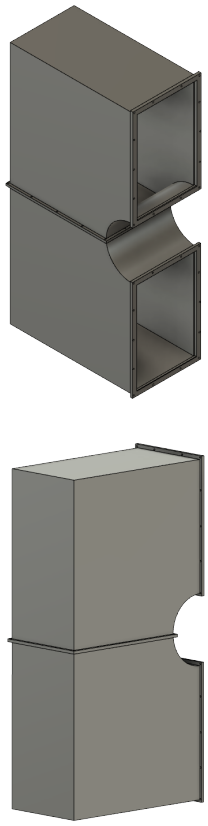

Figure 2.4: Corners 3 and 4

Since these corners maintain the same shape of the chamber of calm, it has been decided to realize the expansion of the return circuit along the vertical plane only. In order to make this possible the other corners must have the same width. To simplify the building phases corners with a square cross-sectional area are designed. Since the side of the square is 1490 *mm*, the area is 2.22 mm^2.

An element of connection between the square corners has to be designed with a height of 745 *mm* in order to realize a symmetrical expansion in the flat-walled diffuser.

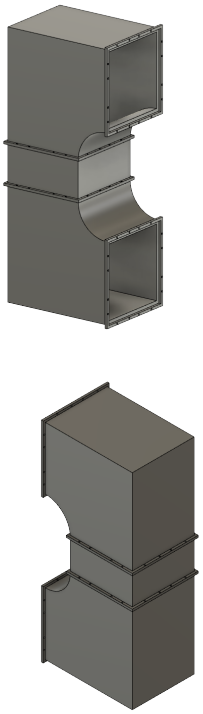

Figure 2.5: Corners 1 and 2

2.2.2 Shape adapter

Between the fan section and the first corner of the return circuit it is necessary to change the shape. This shape adapter is designed to change from a circular cross-section area of 2.545 mm^2 to a square area of 2.22 mm^2. The exit area is less than the entering one realizing a little contraction. This feature allows to have a better control of the flow inside the duct avoiding flow separations along the walls which could happen in shape adaptors.

Shape adapter	
Entering Section	2.545 m^2
Exit section	2.22 m^2
Coeff. of Contraction CR	1.15
Length	3 m
Equivalent conical angle θ_e	2.97 $^\circ$

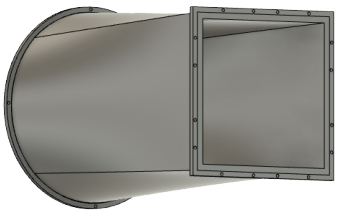

Figure 2.6: Design of the shape adapter

Since the contraction ratio is small it is not necessary to realize the concave-convex shape typical of nozzle. A virtuous geometry could be realize to have a better control of the flow but it will be more expansive and more difficult to build. Thus, for the design of this return circuit a linear contraction is adopted to shape this element.

(a) (b)

Figure 2.7: Two different type of shape possible: a) Simple contraction; b) Concave-convex

2.2.3 Diffuser

The diffuser realizes the expansion of the flow in order to obtain a pressure recovery and minimize the losses of the return circuit. Since the length available is high, there are not problems about separation of the boundary layer of the flow along the internal walls. A flat-walled design concept is realized in order to maximize the pressure recovery. The principal characteristics are summarized in the following table:

Diffuser	
Entering Section	2.22 m^2
Exit section	3.33 m^2
Length	19.98 m
Semiangle θ_e	0.427 $^\circ$

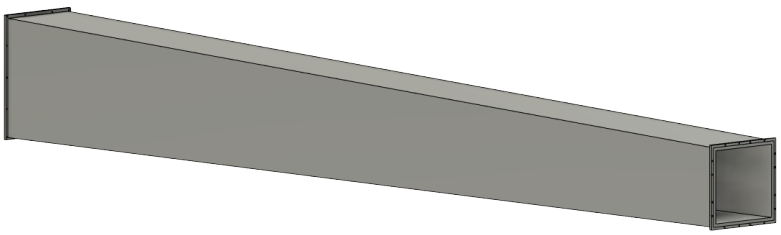

Figure 2.8: Design of the diffuser

2.2.4 Complete design of the return circuit

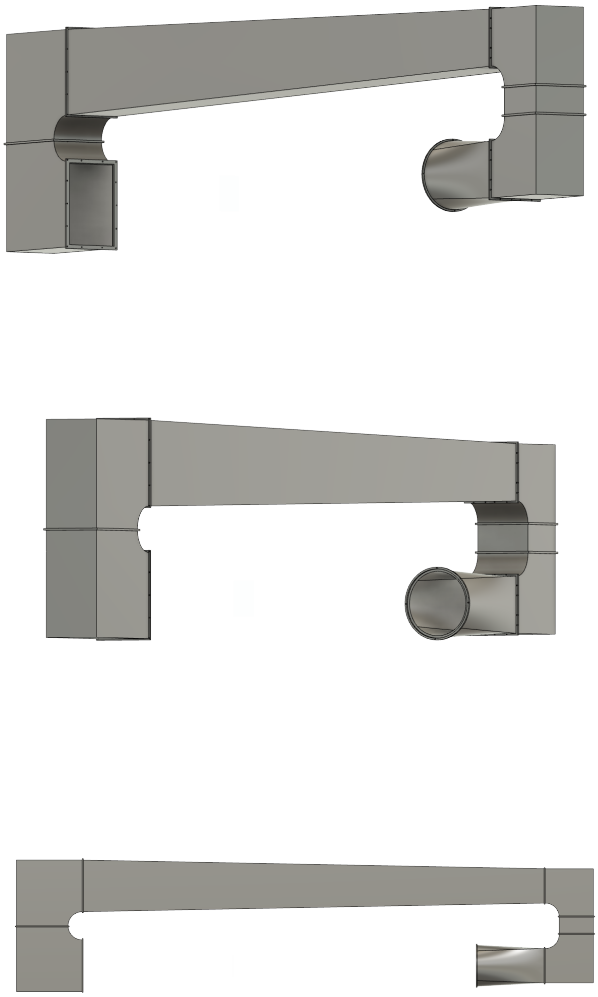

Figure 2.9: Design of the complete design of the return circuit

2.3 Horizontal design

The model here shown has a horizontal development in order to adapt the wind tunnel to a place with a low ceiling. The area occupied by the tunnel is the limit of the project meaning that the distance between the corners and the length development are limited. This situation lead to study the possible arrangement of multiple diffusers in the return circuit because one may have an angle of expansion beyond the critical value. Furthermore a curve corner must be realize.

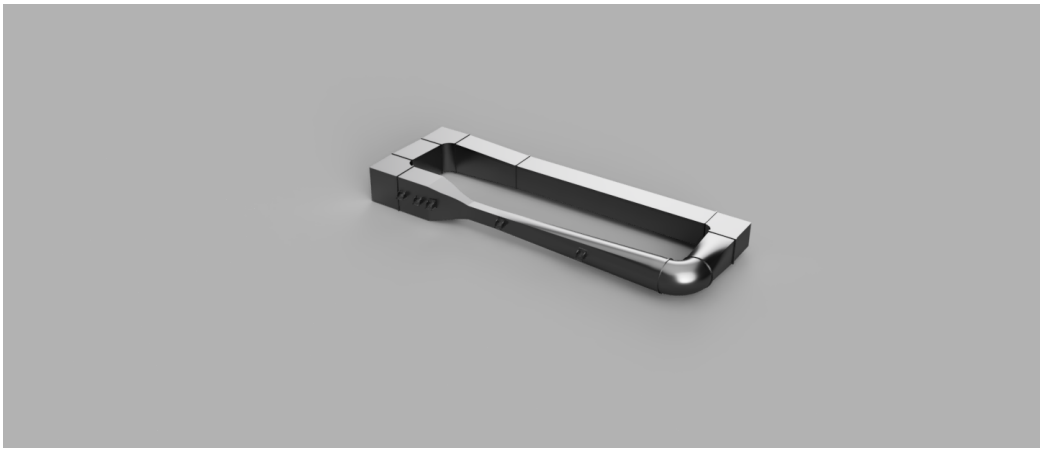

Figure 2.10: Rendering 3D of the close wind tunnel

2.3.1 Corners

To begin with a curve corner must be design to reduce the length of the wind tunnel. This component will be expansive and difficult to realize in a potential building phase.

The design of the following corners was limited by the design of the other components which have leads to the final geometry. In spite of that the common idea behind the design of the corner is to realize them with constant area section and to mantein a rectangular shape with always a side of 1490 *mm* of length as on of the dimension of the chamber of calm. Thanks to this feature flat-walled diffusers could be realized in the return circuit.

Figure 2.11: 3D rendering with the corner with circular area section

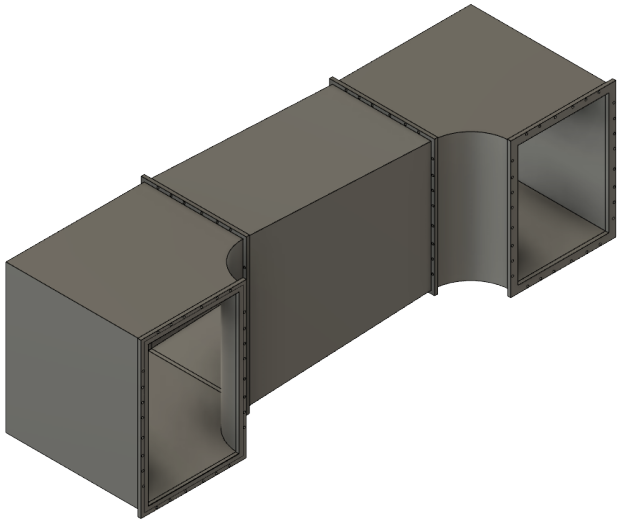

Figure 2.12: Design of last two corners with the diffuser between them

2.3.2 Shape adapter

Between the first corners and the second corner of the return circuit it is necessary to change the shape. This shape adapter is designed to change from a circular cross-section area of 2.545 mm^2 to a square area of 2.22 mm^2. The exit area is less than the entering one realizing a little contraction. This feature allows to have a better control of the flow inside the duct avoiding flow separations along the walls which could happen in shape adaptors. The same consideration about a

more virtuous internal geometry can be designed such as described in paragraph 2.2.2.

Shape adapter	
Entering Section	2.545 m^2
Exit section	2.22 m^2
Coeff. of Contraction CR	1.15
Length	3 m
Equivalent conical angle θ_e	2.97 $^\circ$

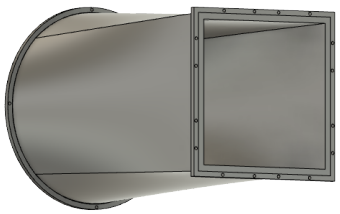

Figure 2.13: Design of the shape adapter

2.3.3 Constant area duct

Between the second and the third corner there is a long section where realize the expansion. Since it is not necessary to realize a long diffuser, a long constant area duct can be designed in order to have an easy object to produce during the building phase and to be the starting point of the project of a second test chamber.

The hydraulic diameter of a test section can be calculated as follow:

$$D_h = 2\sqrt{\frac{A}{\pi}} \tag{2.3}$$

The length of a test section must be included between 0.5 times and 3 times its hydraulic diameter as discussed in the paragraph 1.4.1 of this dissertation.

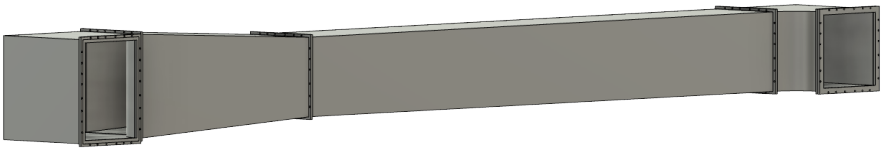

Figure 2.14: Design of the second side of the return circuit with the element of constant cross-sectional area

2.3.4 Diffusers

The diffuser realizes the expansion of the flow in order to obtain a pressure recovery and minimize the losses of the return circuit. A single diffuser between the last two corners cannot be realize: the angle of expansion is beyond the critical value shown in the paragraph 1.4.2 of this dissertation. Flat-waled diffusers are realized in order to simplify an eventual building phase and to reach a better pressure recovery. A good compromise for the design of multiple diffuser is reached iteratively obtaining the following results:

Diffuser 1	
Entering Section	2.22 m^2
Exit section	2.91 m^2
Length	4500 mm
Semiangle θ_e	2.91 $^\circ$

Diffuser 2	
Entering Section	2.91 m^2
Exit section	3.33 m^2
Length	2840 mm
Semiangle θ_e	2.86 °

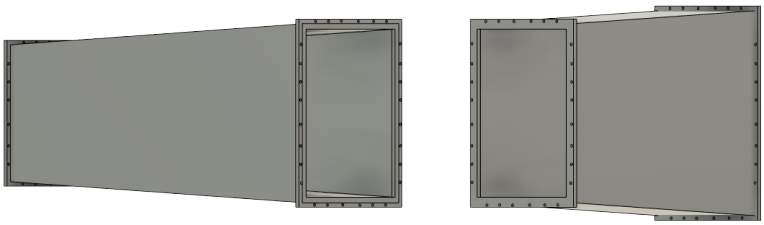

Figure 2.15: Design of the two diffusers

2.3.5 Complete design of the return circuit

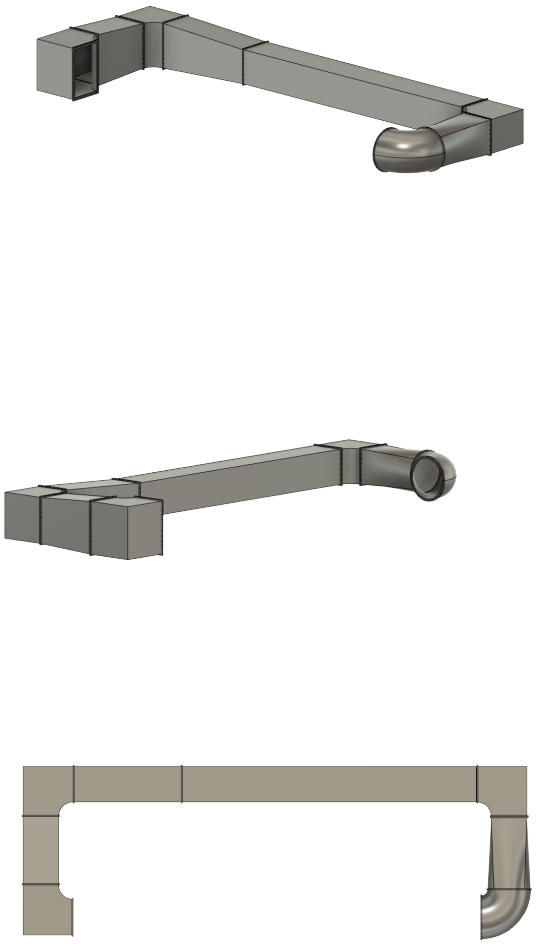

Figure 2.16: Design of the complete design of the return circuit

Chapter 3

Pressure Losses

3.1 Energy Consideration

The conditions at any cross section of a wind tunnel circuit are considered to be represented by the area-weighted average value of the flow parameters over the section. Considering the static pressure p at location c in a wind tunnel circuit that has A as cross-sectional area, we define :

$$p_c = \frac{1}{A_c} \iint_{A_c} p\, dA \tag{3.1}$$

To study the power of a fluid at constant velocity as the one in the test section we can define it in terms of density, test-section area, and test-section flow velocity as the given equation:

$$P_t = \frac{1}{2} \dot{m}_t V_t^2 = \frac{1}{2} \rho_t A_t V_t^3 \tag{3.2}$$

In the reality case the stream has not got an uniformity velocity in every point of the section and the information about the effects of distribution of the velocity could be lost even assuming the main velocity $\bar{V}$. To avoid these problems the coefficient of kinetic energy is introduced by the equation:

$$\alpha = \frac{1}{A\bar{V}^3} \int_A V^3 dA \tag{3.3}$$

Since his low value, this coefficient is often negligible.

The ratio of the power in the test-section flow to the rate of flow losses around the circuit is a measure of the energy efficiency of a wind tunnel. If we denote the

rate of flow losses in the circuit by P_c, using in the denominator the P_t previous defined by Equation (3.2), then the energy ratio can be expressed by

$$E = \frac{P_t}{P_c} \tag{3.4}$$

This definition provides a focus on the aerodynamic aspects of the energy budget and it shows a clear distinction of the circuit flow properties from the efficiency of the driving fan and the electrical or other driving equipment.

3.2 Energy Losses

The losses in a return-type wind tunnel are considered by splitting the tunnel into component parts and analyzing the losses in each component in succession. Typical components are considered as cylindrical sections, corners, expanding sections or diffuser, contracting sections, annular sections, straightener section, and fan. The fan is exceptional since energy is supplied to the stream at that location. A loss of energy occurs in each of the sections except for the fan. There is an energy transformation from mechanical form to heat that results in raising the temperature of the flowing gas and the solid materials with which it is in contact. The energy transformation comes about due to the viscous action between the flowing gas and the solid boundaries. This transformation from mechanical energy to heat is defined as a loss.

For a compressible flow:

1. Bernoulli's equation $p_s + \frac{1}{2}\rho V^2 = p_{tot} = const$. There are always losses in the sections, and one or the other of the two terms at the second part must show a diminution corresponding to the loss in head.

2. Law of continuity $Q = AV = const$. Areas and velocities at the two stations, constrains the velocity, and hence the velocity head or dynamic pressure at the second location cannot decrease.

There will be equal drops in static head and in total head corresponding to the friction loss. Throughout the wind tunnel the losses that occur appear as successive pressure drops to be balanced by the pressure rise through the fan. The total pressure drop ΔH will be the pressure rise required of the fan.

The loss in a section l is defined as the mean loss of total pressure ΔH sustained by the stream in passing through the particular section. The loss in a section is

given in dimensionless form by the ratio of the pressure loss in the section to the dynamic pressure at the entrance to the section. For a typical "local" section this is given by

$$K_l = \frac{\Delta H_l}{1/2\rho_l V_{l2}} = \frac{\Delta H_l}{q_l} \quad (3.5)$$

This definition of loss coefficient is both important and convenient. It is convenient because the total pressure loss and the dynamic pressure are easily measurable quantities. We now consider further its importance. The time rate of energy loss in a section can be expressed as the product of the total pressure loss times the volume rate of flow through the section, $\Delta E_l = A_l V_l \Delta H_l$, which with ΔH_l from Equation (3.5) gives $\Delta E_l = A_l V_l K_l q_l$,and finally

$$\Delta E_l = K_l \left(\frac{1}{2} \dot{m} V_{l2} \right) \quad (3.6)$$

Equation (3.6) shows that the loss coefficient defined by Equation (3.5) on the basis of total pressure loss and dynamic pressure also is the ratio of the rate of energy loss to the rate of flow of kinetic energy into the section. These local losses are referred to the test-section dynamic pressure, defining the coefficient of loss of the local section referred to the test-section dynamic pressure as

$$K_{lt} = \frac{\Delta H_l}{q_l} \frac{q_l}{q_l} = K_l \frac{q_l}{q_l} \quad (3.7)$$

Using the definition of P,as given by Equation (3.3) with Equations (3.5) and (3.6) provides a test-section referenced result:

$$\Delta E_l = K_{lt} \left(\frac{1}{2} \dot{m} V_{l2} \right) = K_{lt} P_t \quad (3.8)$$

The total rate of loss in the circuit is obtained by summing the rate of section losses for each of the individual sections:

$$P_c = \sum_l \Delta E_l = \sum_l \Delta K_{lt} P_t \quad (3.9)$$

The energy ratio as defined by Equation (3.4) can be expressed in terms of the loss coefficients of the various sections as

$$\boxed{E_R = \frac{1}{\sum_l \Delta K_{lt}}} \quad (3.10)$$

As noted previously, this definition of energy ratio excludes the energy losses associated with the fan and the motor. The total rate of loss in the circuit as represented by Equation (3.8) is the net power that the tunnel drive device must deliver to the airstream to maintain steady conditions.

3.3 Constant-area section

Considering a constant-area section, the pressure loss ΔH along the duct is proportional to its length L, the hydraulic diameter D_h, the fluid density ρ, and the square of mean flow velocity U we obtain the following equation where the friction factor f is the constant of proportionality:

$$\frac{\Delta H}{\rho} = f\frac{L}{D_h}\frac{U^2}{2} \tag{3.11}$$

Combining this result with the Equation (3.5) we obtain the loss coefficient of a constant area section:

$$K_l = f\frac{L}{D_h} \tag{3.12}$$

For smooth pipes at high Reynolds numbers there is the Prandtl universal law of friction:

$$\frac{1}{\sqrt{f}} = 2log_{10}\left(Re\sqrt{f}\right) - 0.8 \tag{3.13}$$

The principal parameters that affect the performance of a constant area section in terms of pressure drops distributed along the duct are:

- length l;
- hydraulic diametre $D_H = \frac{4A}{\Pi}$ where Π is the perimeter and A the cross sectional area;
- Reynolds number $Re = \frac{\rho U D_H}{\mu}$;
- relative roughness $\frac{\varepsilon}{D_H}$
- coefficient of frinction λ
- coefficient of correction forn non circular duct K_{non-c}

The coefficient of losses is calculated the equation:

$$K_l = K_{non-c}\lambda\frac{l}{D_H} \tag{3.14}$$

where λ is the coefficient of friction:

$$\lambda = \lambda\left(Re, \frac{\varepsilon}{D_H}\right) \tag{3.15}$$

The value of the coefficient of friction can be found using the Moody diagram (Fig. 3.1) or the Chen's equation:

$$\frac{1}{\sqrt{f}} = -4\log_1 0\left[\frac{1}{3.7065}\left(\frac{\varepsilon}{D_H}\right) - \frac{5.0452}{Re}\log_{10}\left(\frac{1}{2.8257}\left(\frac{\varepsilon}{D_H}\right)^{1.1098} + \frac{5.8506}{Re^{0.8981}}\right)\right] \tag{3.16}$$

The coefficient of friction is related to the friction factor by:

$$\lambda = 4f \tag{3.17}$$

For non circular duct:

$$K_{non-c} = 1.1 - 0.1\frac{a}{b} \tag{3.18}$$

The coefficient of losses here obtained is used not only for the test section of the design models but for other components too, as the fan section, which is considered as empty in this dissertation.

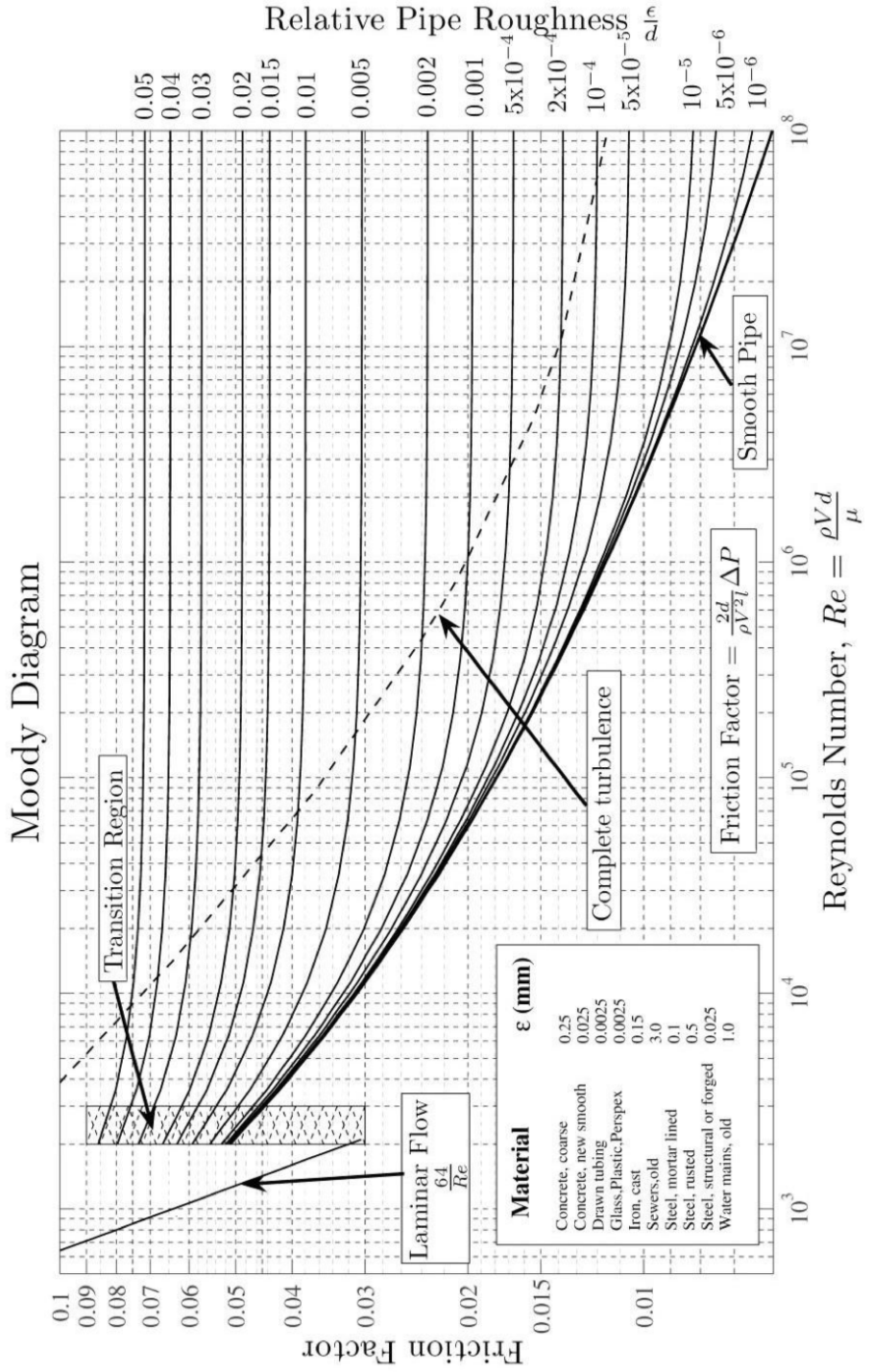

Figure 3.1: Moody diagram

3.4 Diffuser

To calculate pressure loss in a diffuser, the energy loss due to friction at the walls and due to expansion and other must be considered. The main parameters are the equivalent conical expansion angle Θ_e and the ratio between inlet and outlet cross-section areas A_R. The coefficient of losses can be considered as composed of two terms:

$$K_d = K_f + K_{exp} \tag{3.19}$$

Where:

1. For one-dimensional flow, constant friction factor and constant density with the stream we obtain the equation:

$$K_f = \left(1 - \frac{1}{A_{r^2}}\right) \frac{f}{8\sin(\Theta_e)} \tag{3.20}$$

2. The expansion loss coefficient can be calculated with the empirical expression :

$$K_{exp} = K_e(\Theta_e) \left(\frac{A_r - 1}{A_r}\right)^2 \tag{3.21}$$

The term $K_e(\Theta_e)$ can be expressed as a geometrical function. Below are shown the expressions found by W.T. Eckert :

$$K_e = \begin{cases} A_1 + B_1\Theta_e, & 0 < \Theta_e < 1.5^\circ \\ A_2 + B_2\Theta_e + C_2{\Theta_e}^2 + D_2{\Theta_e}^3 + E_2{\Theta_e}^4 + F_2{\Theta_e}^5 + G_2{\Theta_e}^6, & 1.5^\circ < \Theta_e < 5^\circ \\ A_3 + B_3\Theta_e, & \Theta_e > 5^\circ \end{cases} \tag{3.22}$$

Parametre	Circule	Square
A_1	0.1033	0.09623
B_1	-0.02389	-0.004152
A_2	0.1709	0.1222
B_2	-0.1170	- 0.04590
C_2	0.03260	0.02203
D_2	0.001078	0.003269
E_2	-0.0009076	-0.0006145
F_2	-0.00001331	-0.0000280
G_2	0.0001345	0.00002337
A_3	-0.09661	-0.01322
B_3	0.04672	0.05866

Table 3.1: Eckert's K_e parametres for circular and square cross-sections

The lower the equivalent conical expansion angle, the lower the loss.

The pressure recovery is affected by what happens to the stream after it exits the diffuser. This section of constant area is called tailpipe. The value of the coefficient of pressure recovery can be obtain by the map of performance for a diffuser without tailpipe ($C_{pr}^{'}$) and for a diffuser with a tailpipe of length $4D_{H2} < L_d < 8D_{H2}$ ($C_{pr}^{''}$). If the tailpipe exits the limits, the value of C_{pr} can be calulcated as follow:

- for short tailpipes with $L_d < 4D_{H2}$

$$C_{pr} = C_{pr}^{'} + \frac{L_d}{4D_{H2}} \left(C_{pr}^{''} - C_{pr}^{'} \right) \tag{3.23}$$

- for long tailpipes with $L_d > 8D_{H2}$ (with δ coeff. of friction):

$$C_{pr} = C_{pr}^{''} - \lambda \frac{L_d - 8D_{H2}}{D_{H2}} \left(\frac{A_1}{A_2} \right)^2 \tag{3.24}$$

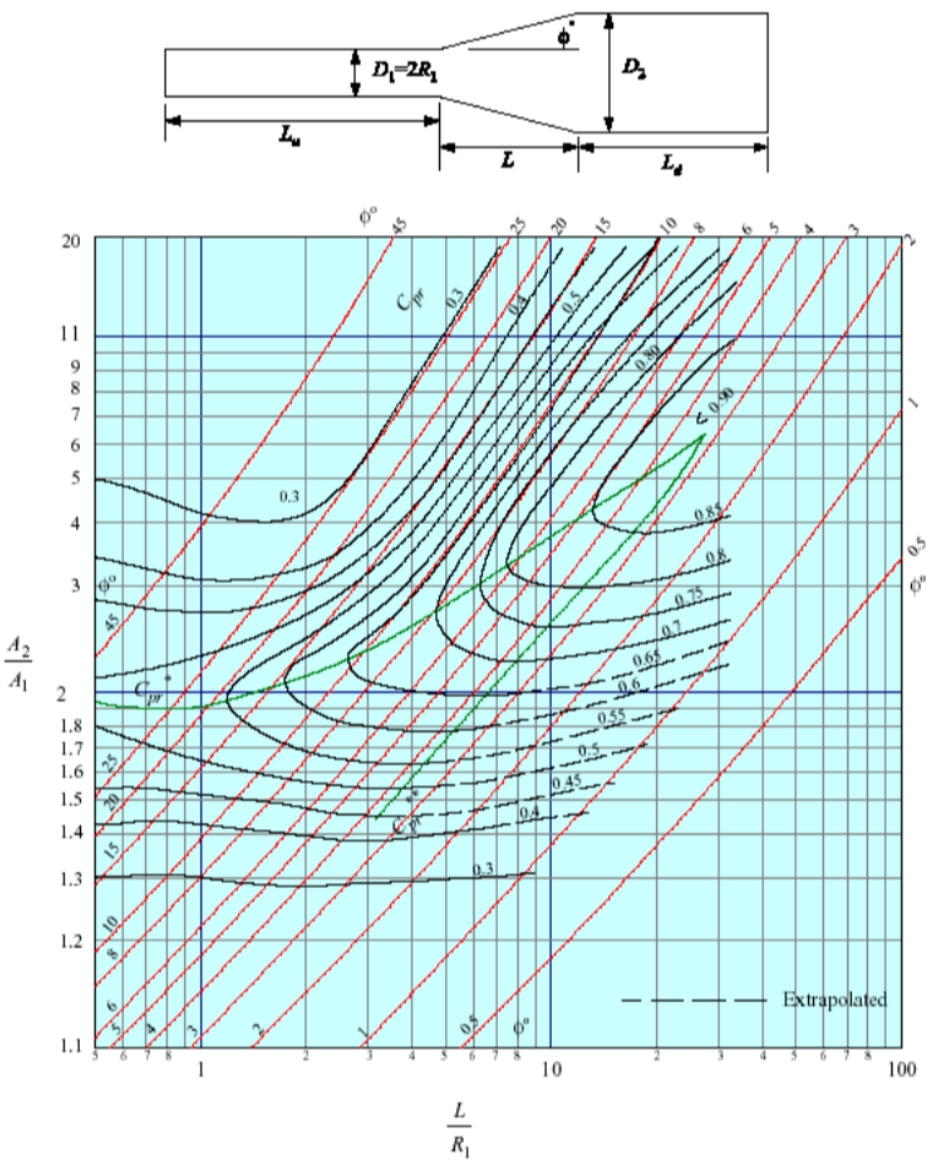

Figure 3.2: Coeff. of pressure recovery for a diffuser with tailpipe such that $4 < L_d/D_{H2} < 8$, extracted from [3]

In addition to this dissertation the coefficient of kinetic energy is used to obtain

an accurate value of the pressure losses. The total pressure can be expressed as:

$$p_{tot} = p_s + \alpha \frac{1}{2} \rho V^2 \tag{3.25}$$

so that the coefficient of losses is given by:

$$K_l = \alpha_l - C_{pr} - \alpha_3 \left(\frac{A_1}{A_2} \right)^2 \tag{3.26}$$

Even if the models have flat diffusers, data from conical' map are used in this dissertation.

3.5 Nozzle

A way to calculate the losses of the nozzle is considering them only caused by friction so that the pressure drop is obtained by integrating the standard pipe friction law:

$$\Delta p_f = \int_0^{L_n} f \frac{\rho}{2} \frac{V_n^2}{D_n} dx \tag{3.27}$$

Combining the Equation (3.5) with the Equation (3.)

$$K_n = f_{av} \left(\frac{L_n}{D_{sc}} \right) \int_0^l \frac{D_{sc}^5}{D_n^5} d \left(\frac{x}{L_n} \right) \tag{3.28}$$

Since the value of the total losses that happens in the nozzle is high since the numbers of dissipative effects which occur inside and the increasing of the velocity, a way more accurate in used. Two terms can be considered: one due to the friction at the walls, the other to the local phenomenons of instability and boundary layer conditions;

$$K_l = K_{fr} + K_{loc} \tag{3.29}$$

For the friction factor is considered as (with the λ and D_h calculated as the average between the entry and the exit) :

$$K_{fr} = K_{non-c} + \bar{\lambda} \frac{L}{\bar{D}_h} \tag{3.30}$$

The local factor is calculated with the approximated equation:

$$K_{loc} = \left(-\frac{0.0125}{CR^4} + \frac{0.0224}{CR^3} - \frac{0.00723}{CR^2} + \frac{0.00444}{CR} - 0.00745 \right) \left(-\theta_e^3 - 2\pi\theta_e^2 - 10\theta_e \right) \tag{3.31}$$

In this dissertation the shape adapter is considered as a nozzle since it realizes a small contraction.

3.6 Corners

To avoid large losses and to maintain relatively straight flow throughout the circuit, the comers are equipped with turning vanes. The corners designed in the two models are of constant area. Expanding corners could be use to obtain a flow of better quality but are more expensive in terms of pressure drops. The shape of turning vanes varies from bent plates to highly cambered airfoils. The first two corners are the most critical in terms of losses owing to higher dynamic pressure.

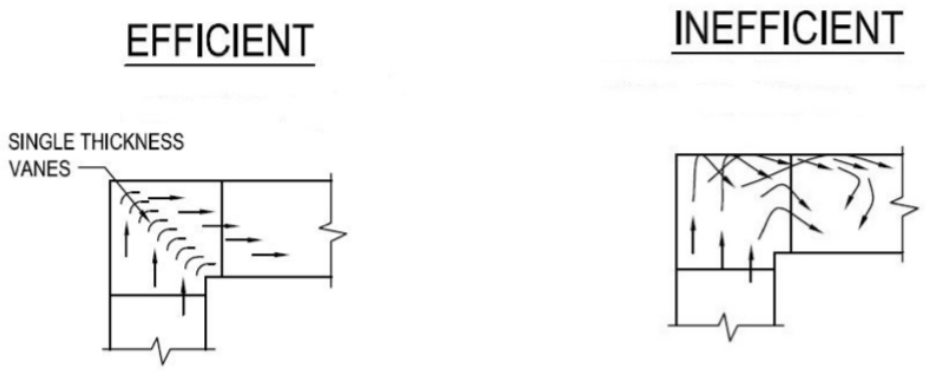

Figure 3.3: Scheme of corners with and without turning vanes, extracted from [4]

The principal parameters are:

- the chord c, which is the distance between the leading edge and the trailing edge
- the gap d, measured between two leading edges
- the pitch $\varepsilon = d/c$

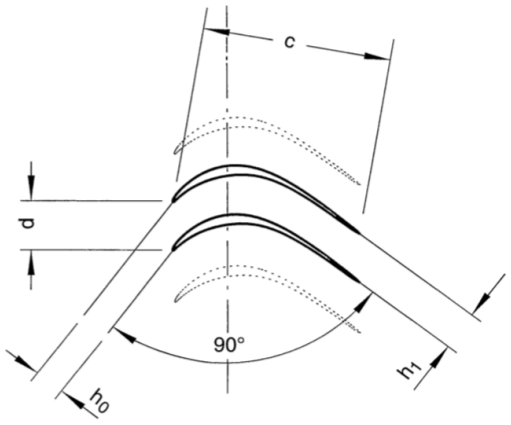

Figure 3.4: Scheme of turning vanes

The losses in the comer vanes can be made small by selecting an efficient cross-sectional shape and by using an appropriate chord-to-gap ratio. Vanes using cambered airfoils and relatively blunt leading edges will be less sensitive to approaching air flow angularities than sharp leading-edge vanes. In this design project a coefficient of losses of $K = 0.036$ was considered by using experimental data from scientific literature.

3.7 Honyecombs

The honeycombs are used in the camber of calm to force the flow to all go in essentially the same direction. They are a guiding device through which the individual air filaments are rendered parallel.

The principal parametres are:

- length l;
- hydraulic diamter of the cells D_{HC};
- width of the cells d;
- Reynolds number $Re = \frac{Ud}{\nu}$;
- porosity $\beta = \left(1 - \frac{d}{M}\right)^2$, where M is the characteristical dimension of the mesh;

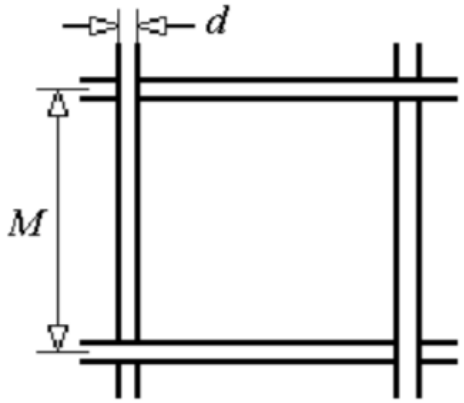

Figure 3.5: Scheme of the mail of honeycombs

The coefficient of losses is calculated as:

$$K_{HC,l} = \delta_{HC}\left(\frac{l_{HC}}{D_{HC}} + 3\right)\left(\frac{1}{\beta}\right)^2 + \left(\frac{1}{\beta} - 1\right)^2 \tag{3.32}$$

where:

$$\delta_{HC} = \begin{cases} 0.375\left(\frac{d}{D_{HC}}\right)^{0.4} Re_d^{-0.1}, & \text{if} Re_d \leq 275 \\ 0.214\left(\frac{d}{D_{HC}}\right)^{0.4}, & \text{if} Re_d \geq 275 \end{cases} \tag{3.33}$$

3.8 Screens

Screens are used in the chamber of calm to bring the various parts of the flow closer to a constant speed. Throughout honeycombs a standard reference velocity is not obtained, but it can be achieved with screens. The flow resistance of a wire screen is approximately proportional to the square of the speed, therefore the resistance in a flow which locally manifests different speeds, is greater at the points of higher speed than at the points of lower speed. Taking into consideration that the final pressure drop is about the same for all stream filaments the result is that the speedier filament expands upon striking the screen, the slower one contracts, and so the speeds become comparable upon passing through the screen.

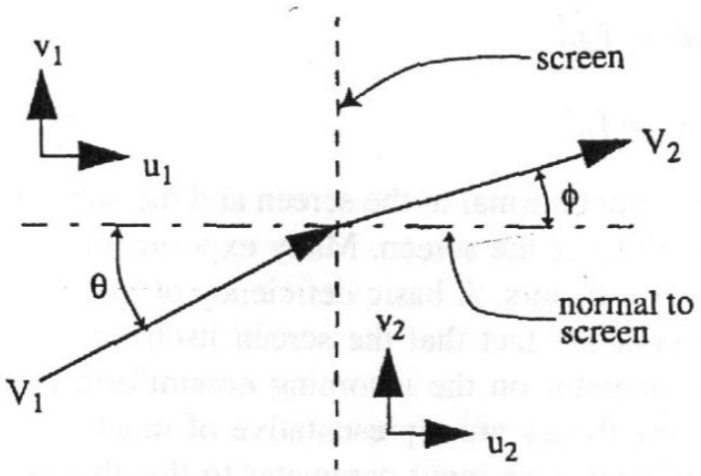

Figure 3.6: Scheme of the flow inside the screens, extracted from [5]

The equation of Laws-Livesey is used to calculate the coefficient of loss:

$$K_{S,l} = A\left(\frac{1}{\beta^2} - 1\right)^B \tag{3.34}$$

where A and B are respectively:

- for quadrangular wires :

$$\begin{cases} A = 0.98 \\ B = 1.09 \end{cases} \tag{3.35}$$

- for circular wires:

$$\begin{cases} A = \begin{cases} \frac{14}{Re_d}, & \text{if} Re_d \leq 10 \\ 0.52 + \frac{66}{Re_d^{4/3}}, & \text{if} 40 \leq Re_d \leq 10^5 \end{cases} \\ B = 1.00 \end{cases} \tag{3.36}$$

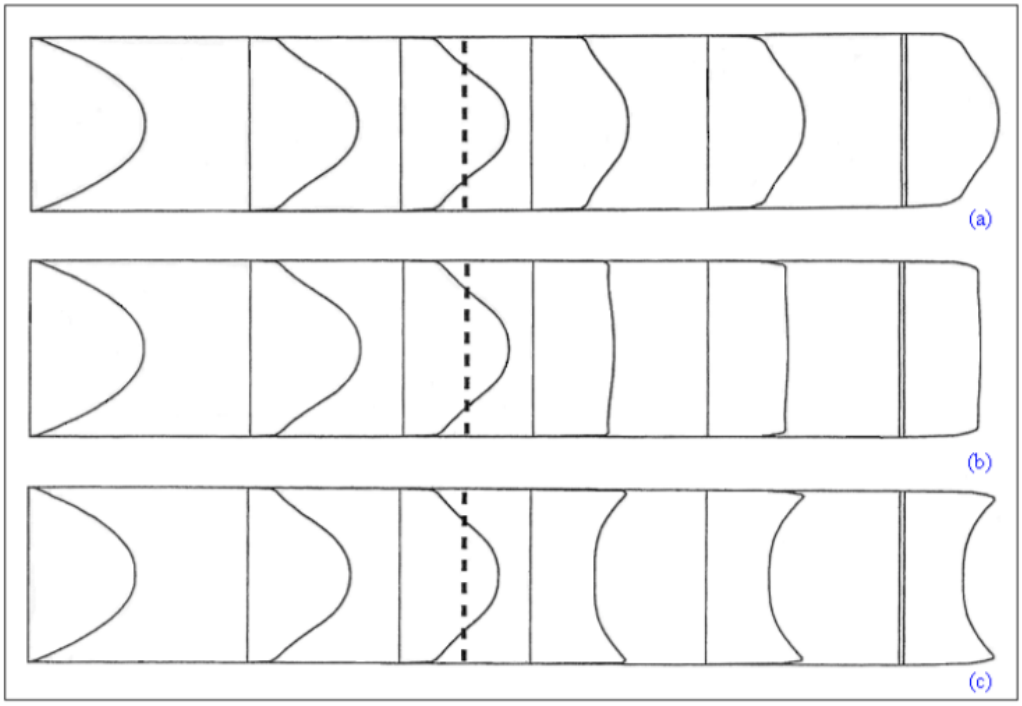

Figure 3.7: Scheme of the evolution of the velocity distribution inside the screen with the variance of the porosity; a) $\beta = 0,75$, $K_l = 0.5$; b) $\beta = 0,53$, $K_l = 2$ c) $\beta = 0.20$, $K_l = 15$, extracted from [3]

In Fig. 3.5. (a) the porosity is high and the coefficient of loss is low; this situation is a compromise and it is used in a lot of wind tunnels. In Fig. 3.5.b) the flow is almost homogeneous but the pressure drops are high besides having the possibility of phenomenons of instability. The worst case is Fig. 3.5.c : the profile of velocity is inverse (overshoot).

3.9 Total losses

The total losses were calculated using a program in Matlab. Pressure and velocity distribution are shown too to better understand the behaviour of the stream inside the wind tunnel. The fan section was considered as empty to have a study focused on the new elements in order to visualize better how the air behaves in the return circuit.

3.9.1 Vertical design

Component	Coeff. of losses
Test section	0.0248
Diffuser	0.1469
Fan section	0.0034
Shape adapter	0.0093
Corner 1	0.002
Leg	0.0057
Corner 2	0.002
Diffuser 2	0.0157
Corner 3	0.0009
Corner 4	0.0009
Chamber of calm (Honeycombs, screens)	0.0851
Nozzle	0.0498

Table 3.2: Total coefficient of losses

The power factor is 0.34654 and the power required to have a velocity of $50 m/s$ in the test section is 14.09 kW. Considering a fan efficiency of $\eta = 0.7$, the fan power is 20.13 kW.

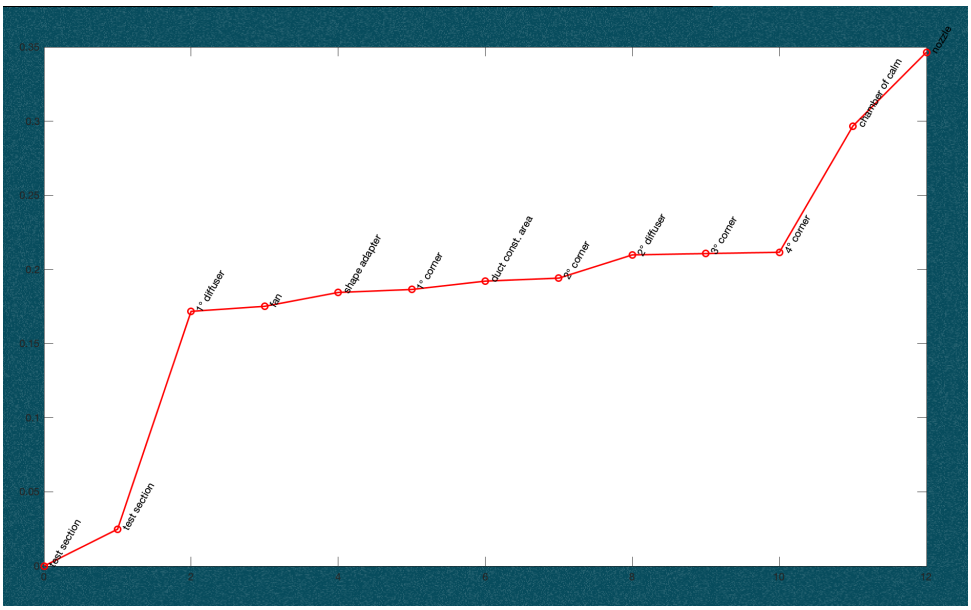

Figure 3.8: Total losses

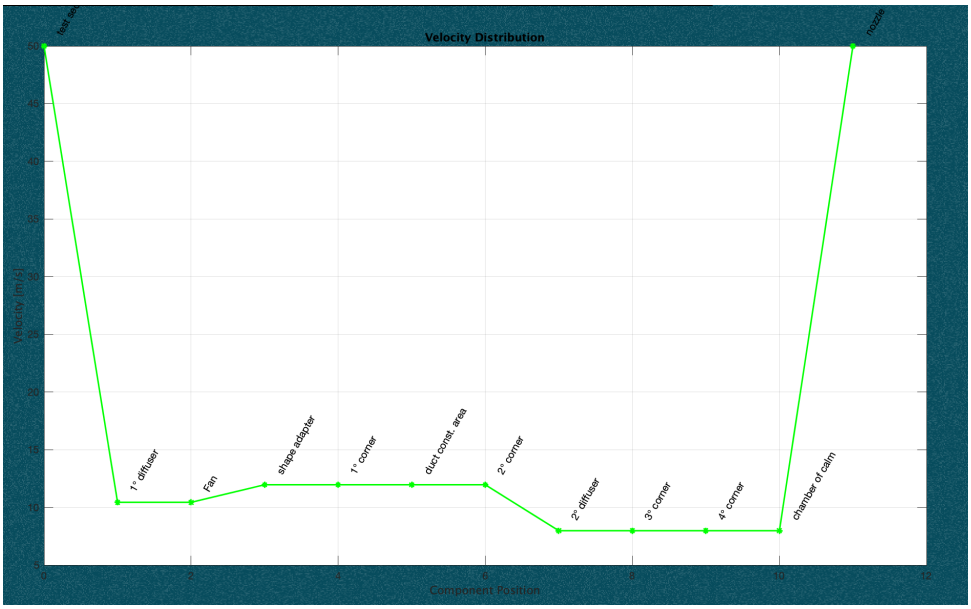

Figure 3.9: Velocity distribution

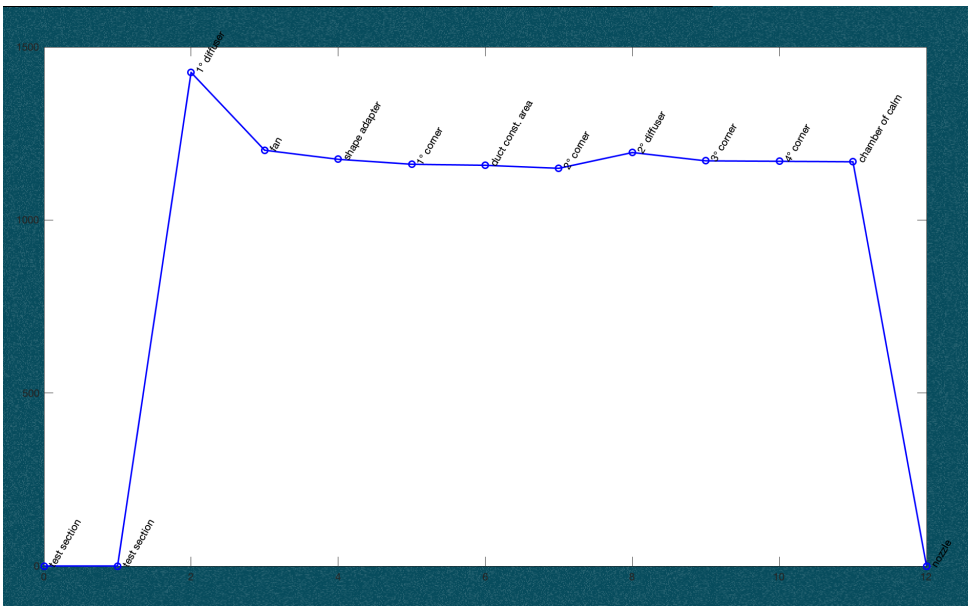

Figure 3.10: Static pressure

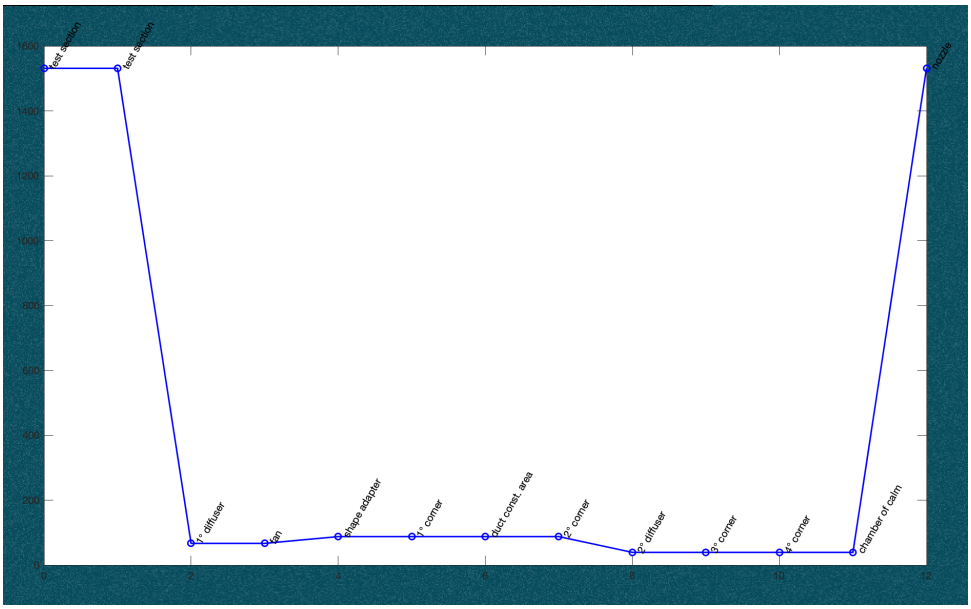

Figure 3.11: Dynamic pressure

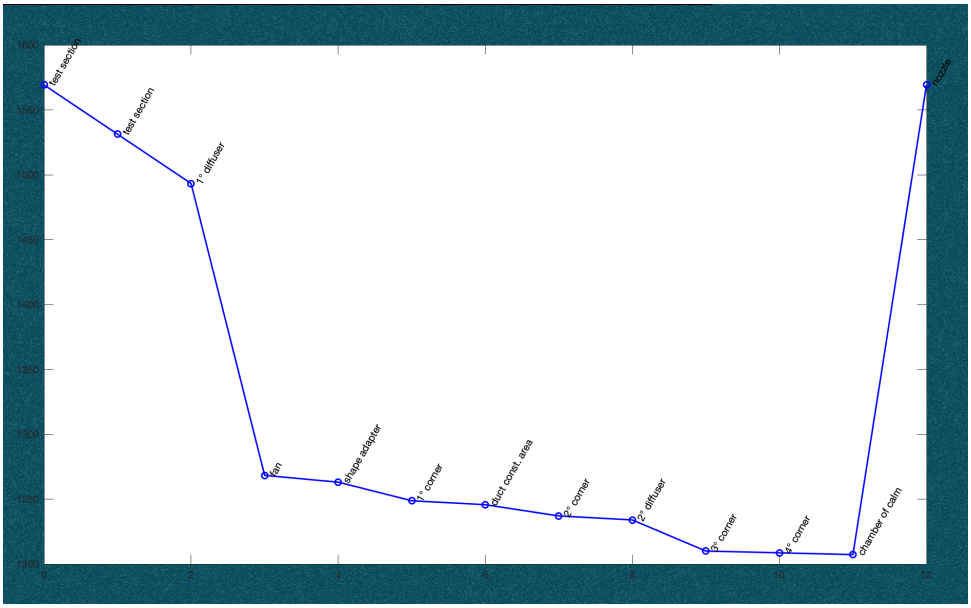

Figure 3.12: Total pressure

3.9.2 Horizontal design

Component	Coeff. of losses
Test section	0.0248
Diffuser	0.1469
Fan section	0.0034
Corner 1	0.0015
Shape adapter	0.0093
Corner 2	0.002
Leg	0.00934
Diffuser 1	0.0046
Corner 3	0.0012
Diffuser 2	0.0011
Corner 4	0.0009
Chamber of calm (Honeycombs, screens)	0.0851
Nozzle	0.0498

Table 3.3: Total coefficient of losses

The power factor is 0.43 and the power required to have a velocity of $50 m/s$ in the test section is 17.32 kW. Considering a fan efficiency of $\eta = 0.7$, the fan power is 24.75 kW.

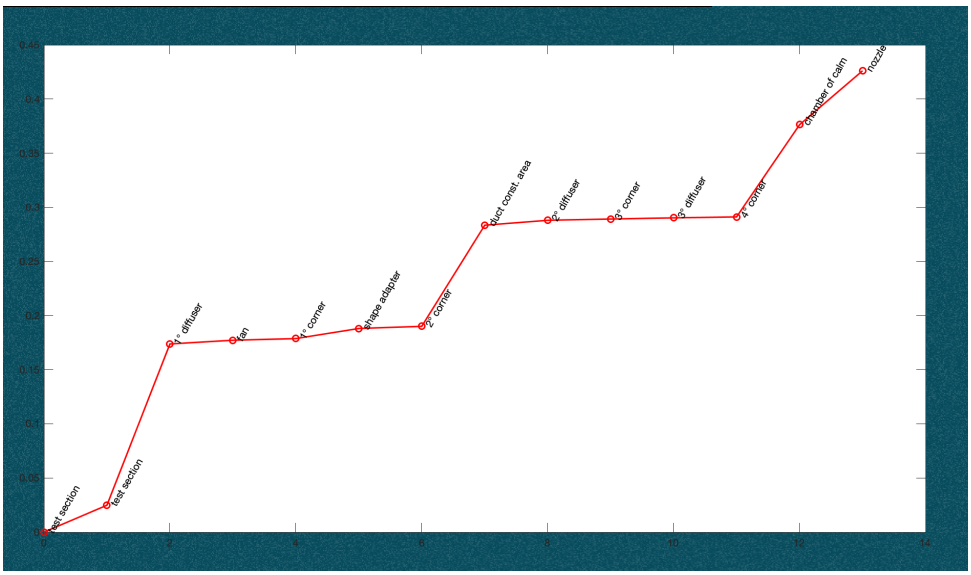

Figure 3.13: Total losses

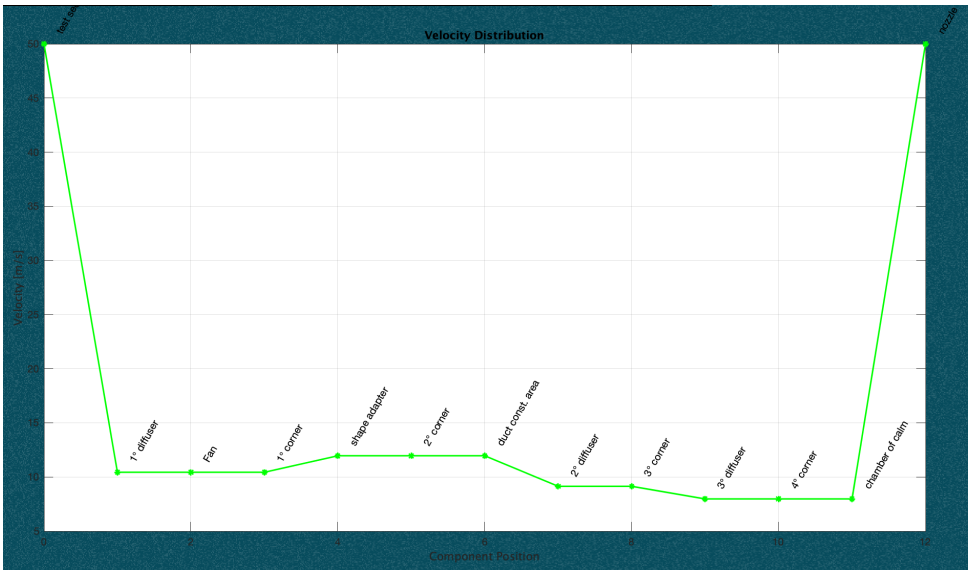

Figure 3.14: Velocity distribution

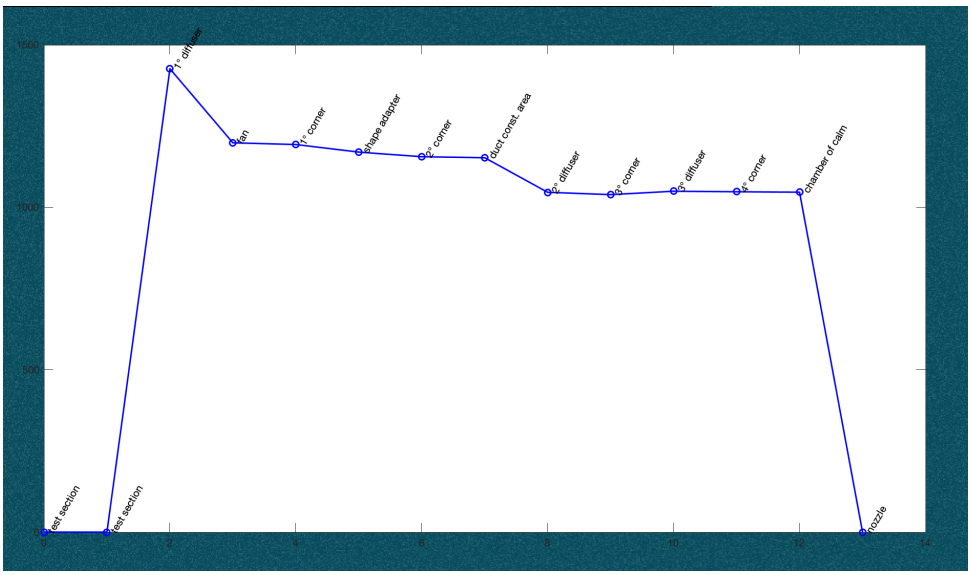

Figure 3.15: Static pressure

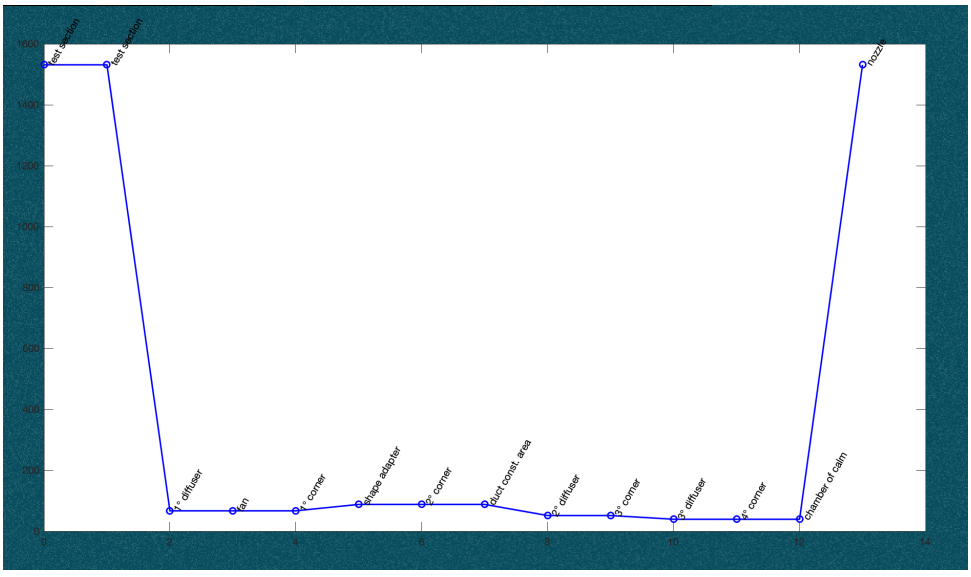

Figure 3.16: Dynamic pressure

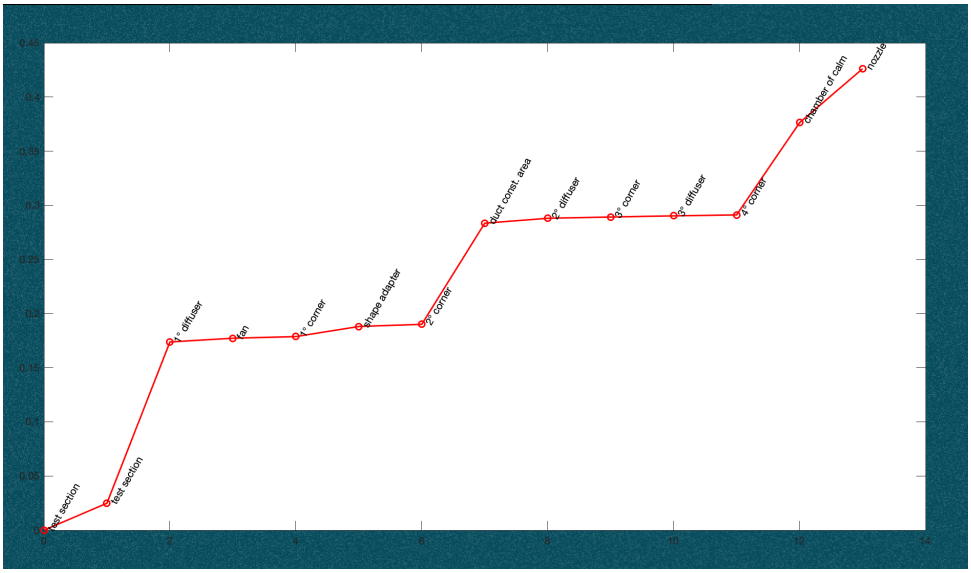

Figure 3.17: Total pressure

Chapter 4

Conclusions

Using the data and the results about wind tunnels present in the scientific literature, a design of the return circuit was possible. The results here shown represent the main design of the constitutive element of a closed loop wind tunnel. A detailed design can follow the models in order to have a better study of the flanges and how to connect the return circuit with the current open loop wind tunnel placed in the laboratory of aerodynamics of the university of Bologna. The results of the analysis of the coefficient of pressure losses show that the best solution in terms of power is the model with vertical development. This means that using the same fan of the current open loop tunnel in a return circuit with vertical development, the velocity reached in the test section is higher than using it in the model with horizontal development. Since the horizontal design solution have one diffuser more than the vertical model and a circular corner, this solution is the most expensive too.

Bibliography

[1] J. D. Pereira, *Wind Tunnels : Aerodynamics, Models and experiments*. Nova Science Publishers, Inc., 2011.

[2] F. M. White, *Fluid mechanics —7th ed.* Mcgraw-Hill series in mechanical engineering, 2011.

[3] F. Spalla, *Progetto Aerodinamico di una Galleria del Vento Subsonica*. Elaborato di Laurea, Università di Bologna.

[4] "https://buildingengineer.wordpress.com," tech. rep., 2011.

[5] J. A. P. Jewel B. Barlow William H. Rae, *Low-Speed Wind Tunnel Testing*. Wiley-Interscience, 1999.

[6] Y. Fuh-Min Fang, J.C.Chen, "Experimental and analytical evaluation of flow in a square-to-square wind tunnel contraction," tech. rep., Department of Civil Engineering, National Chung-Hsing University, 250 Kuo-Kuang Road, Taichung 40227, Taiwan, 2001.

[7] J. D. Anderson, *Fundamentals of aerodynamics*. New York: McGraw-Hill, 2011.

[8] P. H. A. Alessandro Talamelli, Antonio Segalini, *Laboratory of Aerodynamics*. Notes for a joint laboratory exercise UNIBO - KTH, 2020.

[9] L. R. F. F. G. A. M. M. Mauro S., Brusca S., "Small-scale open-circuit wind tunnel: Design criteria, construction and calibration," tech. rep., Department of Civil Engineering and Architecture, University of Catania, 2017.

[10] J. H. Bell and R. D. Mehta, "Contraction design for small low-speed wind tunnels," tech. rep., Department of Aeronautics and Astronautics Stanford University Stanford, CA 94305, 1988.

Appendix A

Vertical design

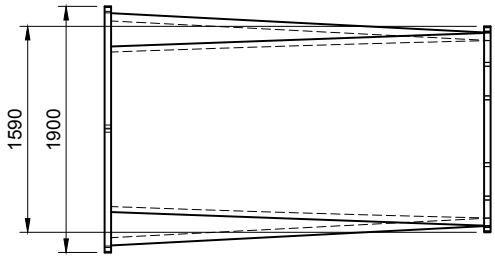

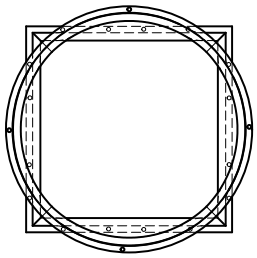

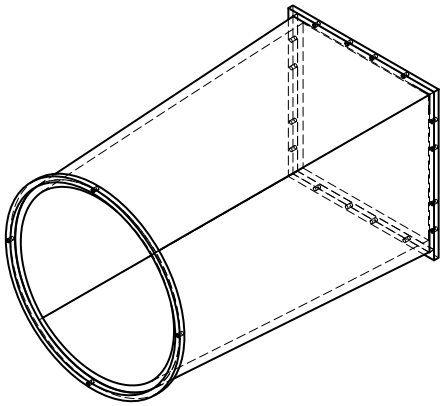

Dept.	Technical reference	Created by	Approved by
		Edoardo Foschi	
		Document type	Document status
		Title	DWG No.
		Shape adapter	
			Rev. / Date of issue / Sheet: 1/1

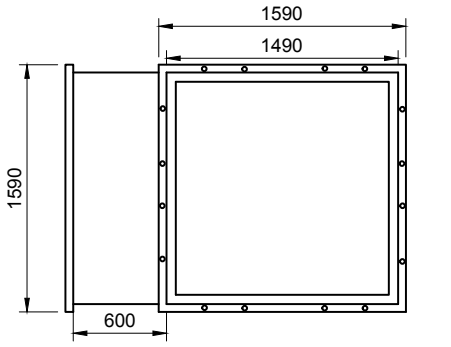

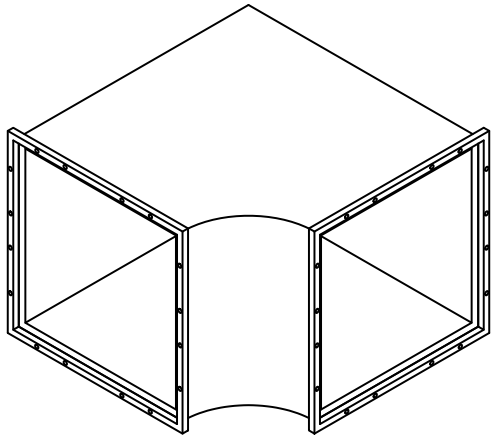

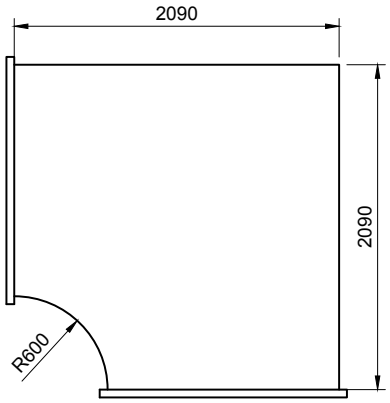

Dept.	Technical reference	Created by	Approved by
		Edoardo Foschi	
		Document type	Document status
		Title	DWG No.
			Rev. / Date of issue / Sheet: 1/1

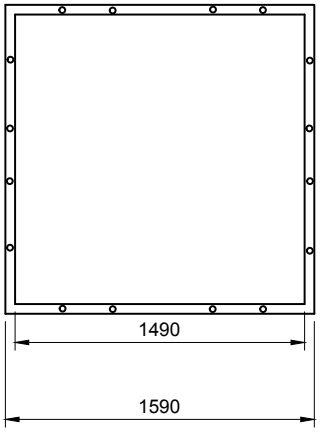

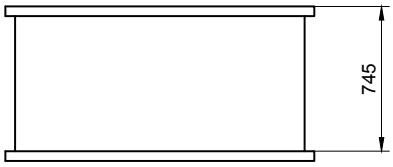

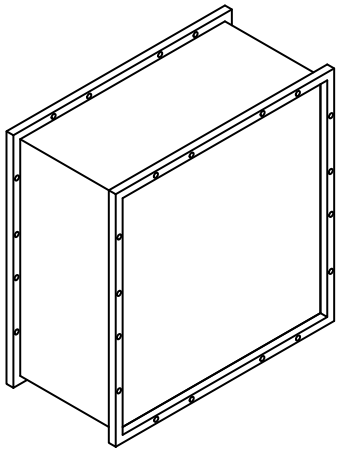

Dept.	Technical reference	Created by	Approved by
		Edoardo Foschi	
		Document type	Document status
		Title	DWG No.
			Rev. / Date of issue / Sheet: 1/1

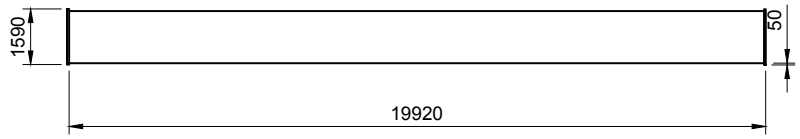

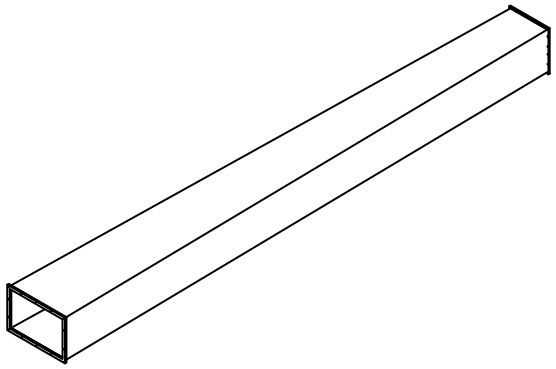

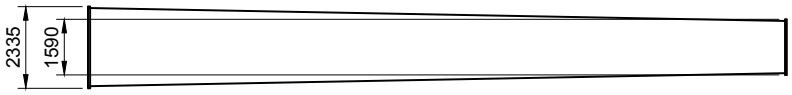

Dept.	Technical reference	Created by	Approved by
		Edoardo Foschi	
		Document type	Document status
		Title	DWG No.
		DIFFUSER	
		Rev.	Date of issue / Sheet
			1/1

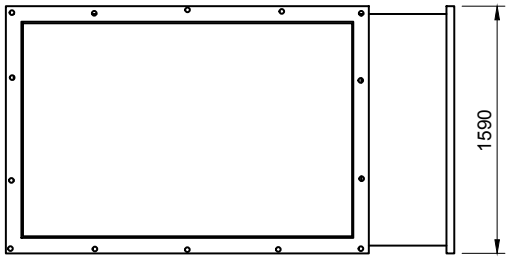

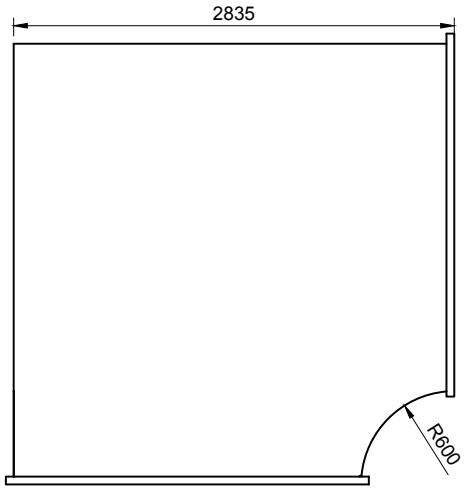

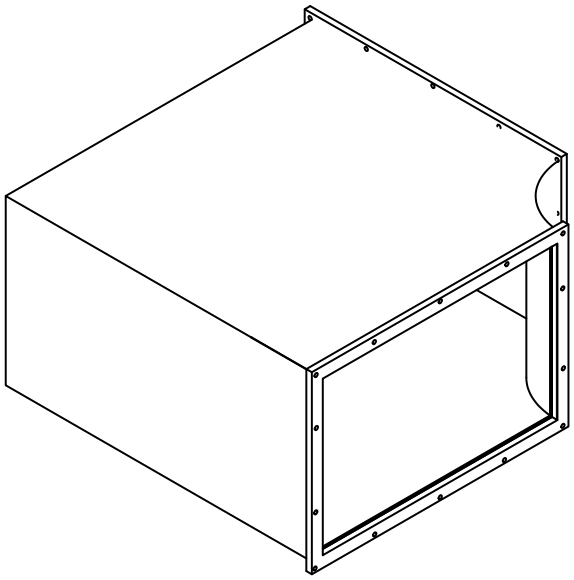

Dept.	Technical reference	Created by	Approved by
		Edoardo Foschi	
		Document type	Document status
		Title	DWG No.
			Rev. / Date of issue / Sheet: 1/1

Appendix B

Horizontal design

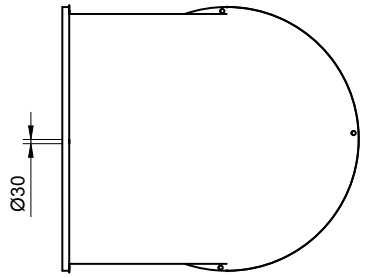

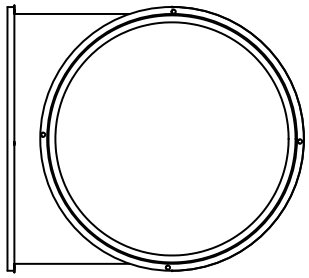

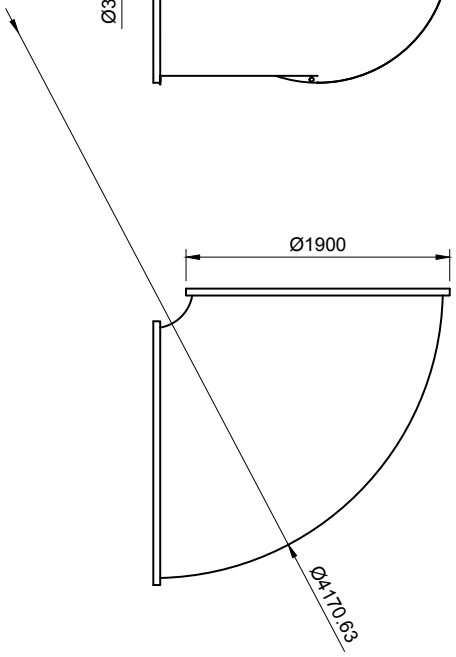

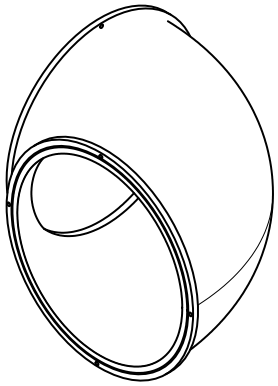

Dept.	Technical reference	Created by	Approved by
		Edoardo Foschi	
		Document type	Document status
		Title	DWG No.
		CORNER 1	
		Rev. / Date of issue	Sheet
			1/1

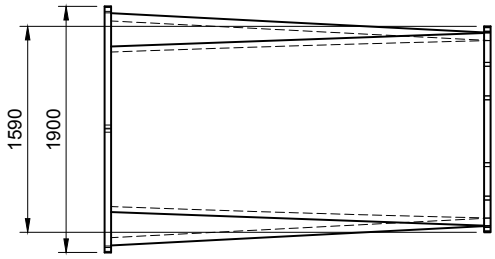

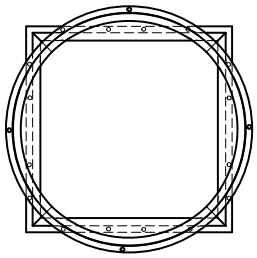

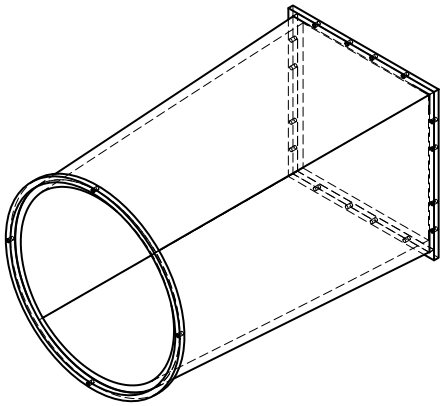

Dept.	Technical reference	Created by	Approved by
		Edoardo Foschi	
		Document type	Document status
		Title	DWG No.
		Shape adapter	
			Rev. / Date of issue / Sheet: 1/1

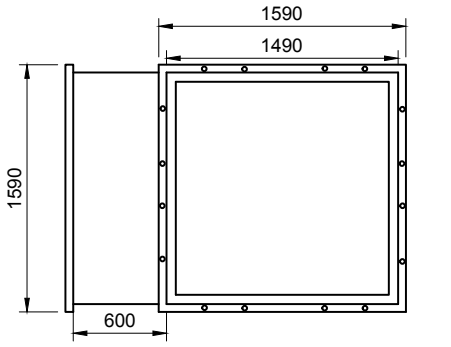

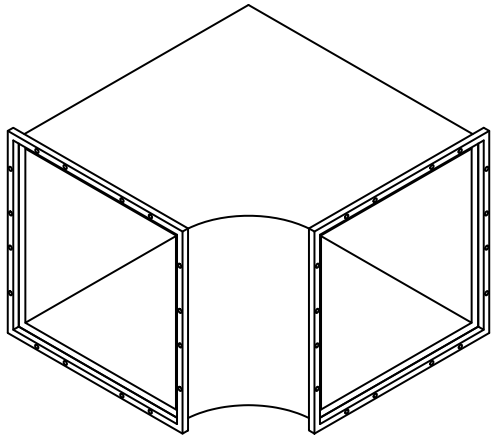

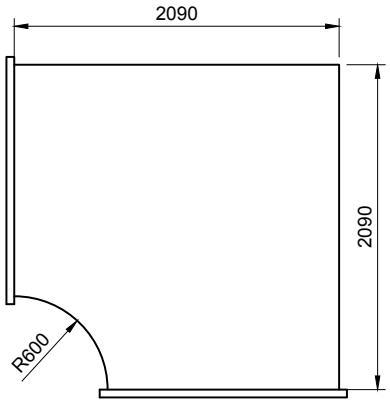

Dept.	Technical reference	Created by	Approved by
		Edoardo Foschi	
		Document type	Document status
		Title	DWG No.
			Rev. / Date of issue / Sheet: 1/1

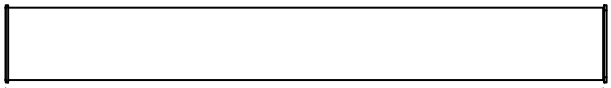

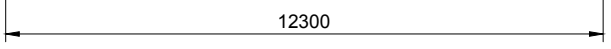

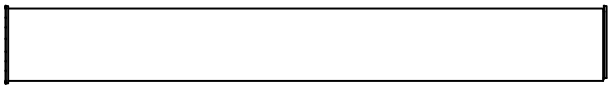

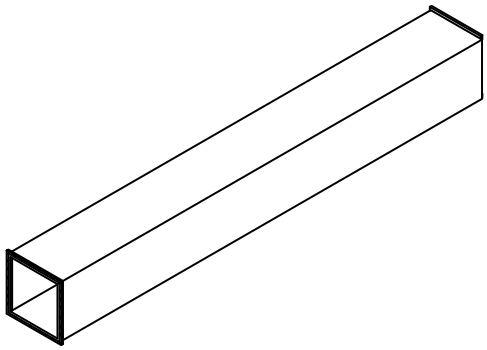

Dept.	Technical reference	Created by	Approved by
		Edoardo Foschi	
		Document type	Document status
		Title	DWG No.
			Rev. / Date of issue / Sheet: 1/1

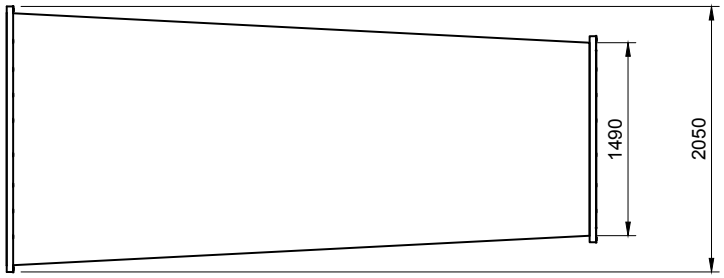

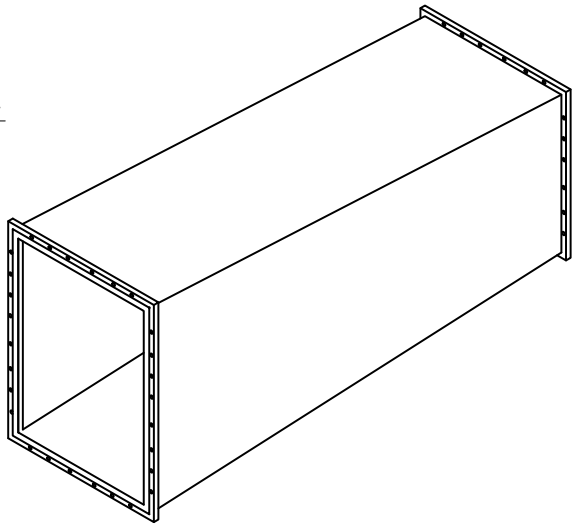

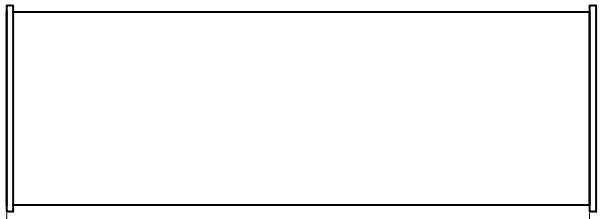

Dept.	Technical reference	Created by	Approved by
		Edoardo Foschi	
		Document type	Document status
		Title	DWG No.
		DIFFUSER 1	
			Rev. / Date of issue / Sheet: 1/1

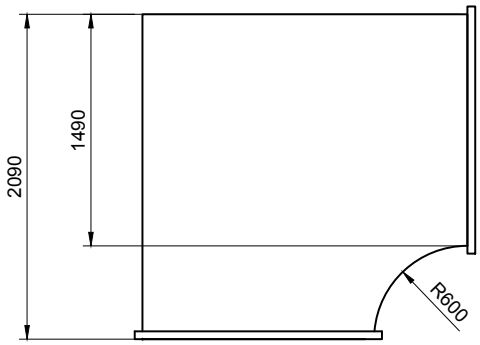

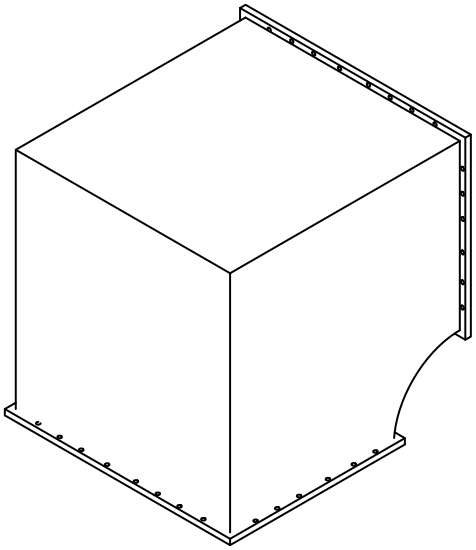

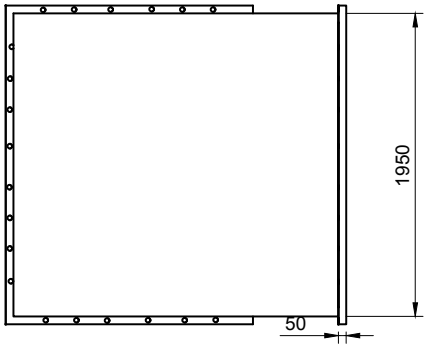

Dept.	Technical reference	Created by	Approved by
		Edoardo Foschi	
		Document type	Document status
		Title	DWG No.
		CORNER 3	
			Rev. / Date of issue / Sheet: 1/1

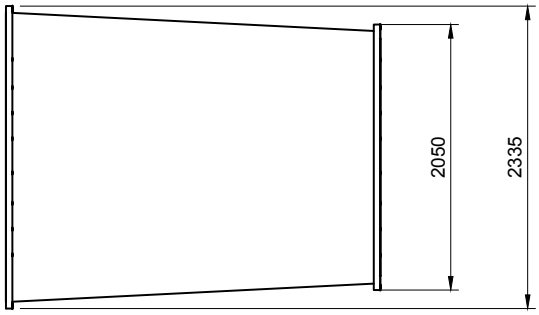

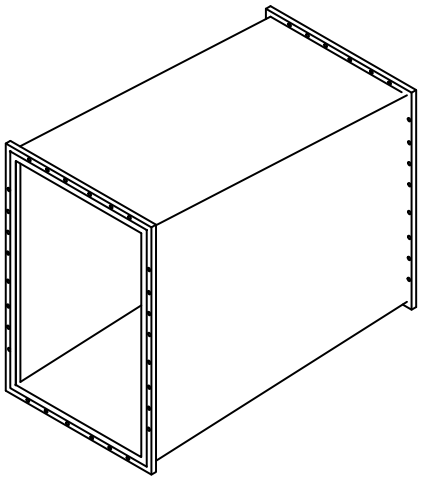

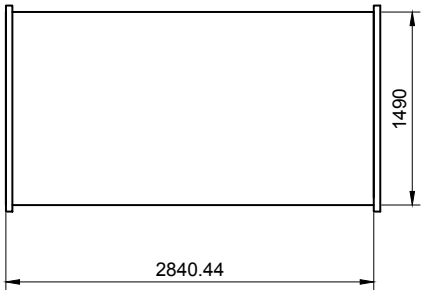

Dept.	Technical reference	Created by	Approved by
		Edoardo Foschi	
		Document type	Document status
		Title	DWG No.
		DIFFUSER 2	
		Rev.	Date of issue / Sheet
			1/1

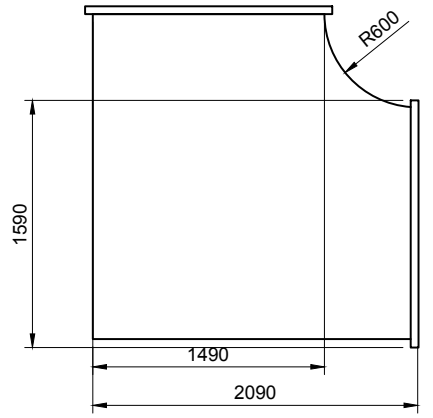

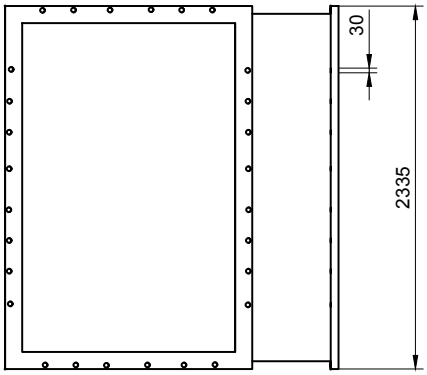

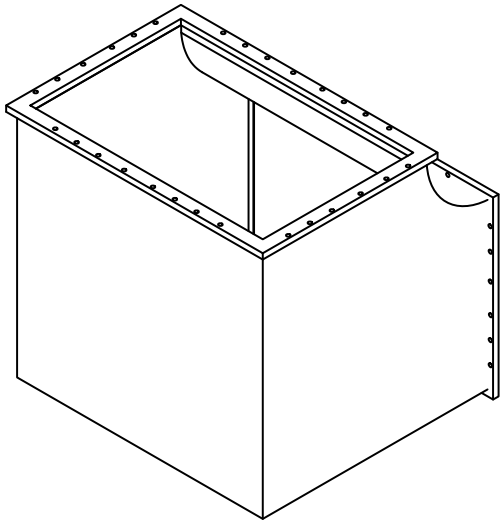

Dept.	Technical reference	Created by	Approved by
		Edoardo Foschi	
		Document type	Document status
		Title	DWG No.
		CORNER 4	
		Rev. / Date of issue	Sheet
			1/1